

2016

Effects of Chemical Structure of Anionic Surfactants on the Wettability of a Carbonate System

Sandeep Gupta

Louisiana State University and Agricultural and Mechanical College

Follow this and additional works at: https://digitalcommons.lsu.edu/gradschool_theses



Part of the [Petroleum Engineering Commons](#)

Recommended Citation

Gupta, Sandeep, "Effects of Chemical Structure of Anionic Surfactants on the Wettability of a Carbonate System" (2016). *LSU Master's Theses*. 297.

https://digitalcommons.lsu.edu/gradschool_theses/297

This Thesis is brought to you for free and open access by the Graduate School at LSU Digital Commons. It has been accepted for inclusion in LSU Master's Theses by an authorized graduate school editor of LSU Digital Commons. For more information, please contact gradetd@lsu.edu.

EFFECTS OF CHEMICAL STRUCTURE OF ANIONIC SURFACTANTS ON
THE WETTABILITY OF A CARBONATE SYSTEM

A Thesis

Submitted to the Graduate Faculty of the
Louisiana State University and
Agricultural and Mechanical College
in partial fulfillment of the
requirements for the degree of
Master of Science in Petroleum Engineering.

in

The Craft and Hawkins Department of Petroleum Engineering

by
Sandeep Gupta
B.E., Manipal Institute of Technology, 2012
August 2016

This work is dedicated to my parents who have always been a pillar of support to me and my professor who guided and mentored me through this journey.

ACKNOWLEDGEMENTS

I would like to sincerely thank Dr. Rao for his belief in me and unwavering support. I am deeply grateful to him for entrusting me with this project and guiding me through and through. I would also like to thank Dr. Mileva Radonjic and Dr. Babak Akbari for so graciously agreeing to be a part of my committee. I am also grateful to Greg Trahan, Dan Plummer and the Sasol team for their valuable support. I would also like to extend my extreme gratitude to my friends from LSU who over time have become more like my family. I really appreciate having them in my life and would like to sincerely thank all of them, especially Paulina Mwangi, Catalina Posada, Juan Felipe Bautista, Jack Rayner Blears, John Whitehead, Valentina Rosasco, Anali Riquer, Erin McCreery, Foad Haeri and Mohammad Al Riyami. Last but definitely not the least, I would like to thank my beautiful family. My mom Dipti Gupta, my dad Dr. S. K. Gupta and Leo. This work is dedicated to them.

TABLE OF CONTENTS

ACKNOWLEDGEMENTS	iii
LIST OF TABLES	vi
LIST OF FIGURES	vii
ABSTRACT	x
1. INTRODUCTION	1
2. LITERATURE REVIEW	4
2.1 Surfactant Structure, Type and Micelle formation	4
2.2 Effect of Surfactants on Interfacial Tension	6
2.3 Structural Effects of Surfactant on Interfacial Tension	7
2.4 Wettability Alteration and Contact Angle Measurement.....	9
2.5 Structural Effects of Surfactants on Wettability-.....	13
3. EXPERIMENTAL APPARATUS AND MATERIALS.....	18
3.1 Materials	18
3.1.1 Rocks.....	18
3.1.2 Fluids and Chemicals.....	18
3.1.3 Surfactants.....	19
3.2 Experimental Apparatus.....	20
3.2.1 DDDC Ambient Cell.....	20
3.2.2 Rock cutting and Soxhlet cleaning system	21
4. RESULTS AND DISCUSSION.....	23
4.1 Wettability determination of Yates oil-Yates brine-limestone system at ambient condition.....	23
4.2 Initial Trials.....	25
4.2.1 Injection of 500 ppm of ALFOTERRA S23-7S 90	25
4.2.2 Injection of 500 ppm of ALFOTERRA S23-13S 90M.....	28
4.2.3 Injection of 1000 ppm of SOLOTERRA 960	29
4.2.4 Conclusion from initial trials	29
4.3 Effect of injection of Alkyl-Alkoxy Sulfates (ALFOTERRA) at a concentration of 100ppm.....	30
4.3.1 ALFOTERRA G16-20S M (Hydrophobicity Rank: 1, $PO(m) = 20$, $EO(n) = 0$) .	30
4.3.2 ALFOTERRA S23-13S 90 (Hydrophobicity Rank: 2, $PO(m) = 13$, $EO(n) = 0$) .	30

4.3.3	ALFOTERRA S23-11S 90 (Hydrophobicity Rank: 3, PO(<i>m</i>) = 11, EO(<i>n</i>)= 0) .	33
4.3.4	ALFOTERRA S23-9S 90 (Hydrophobicity Rank: 4, PO(<i>m</i>) = 9, EO(<i>n</i>)= 0)	35
4.3.5	ALFOTERRA S23-7S 90 (Hydrophobicity Rank: 5, PO(<i>m</i>) = 7, EO(<i>n</i>)= 0)	38
4.3.6	ALFOTERRA K3-41S (Hydrophobicity Rank: 6, PO(<i>m</i>) = 4, EO(<i>n</i>)= 1).....	40
4.3.7	ALFOTERRA K45-DS (Hydrophobicity Rank: 7, PO(<i>m</i>) = 0, EO(<i>n</i>)= 3).....	41
4.4	Interfacial tension measurements of ALFOTERRA.....	42
4.5	Effect of injection of Alkyl Ether Carboxylates (SOLOTERRA) at a concentration of 100 ppm	45
4.5.1	SOLOTERRA 960 (Hydrophobicity Rank: 1, PO(<i>m</i>) = 4.5, EO(<i>n</i>)= 2)	45
4.5.2	SOLOTERRA 961 (Hydrophobicity Rank: 2, PO(<i>m</i>) = 4.5, EO(<i>n</i>)= 5)	46
4.5.3	SOLOTERRA 939 (Hydrophobicity Rank: 3, PO(<i>m</i>) = 1.6, EO(<i>n</i>)= 2.4)	47
4.5.4	SOLOTERRA 970 (Hydrophobicity Rank: 4, PO(<i>m</i>) = 3, EO(<i>n</i>)= 7)	49
4.5.5	SOLOTERRA 938 (Hydrophobicity Rank: 5, PO(<i>m</i>) = 0, EO(<i>n</i>)= 7)	50
4.6	Interfacial Tension Measurements for SOLOTERRA.....	52
4.7	Bond number (N_B) analysis during surfactant injection	55
4.8	Summary of results and observations	63
5.	CONCLUSIONS AND RECOMMENDATIONS.....	71
5.1	Conclusions.....	71
5.2	Recommendations.....	74
	REFERENCES	75
	VITA.....	79

LIST OF TABLES

Table 1: Composition of Yates synthetic brine.....	18
Table 2: Dynamic Water Advancing Contact angle as measured for initial system	24
Table 3: Dynamic Water Advancing Contact Angle for various times during injection of 500 ppm of ALFOTERRA S23-7S 90M.	26
Table 4: Dynamic Water Advancing Contact Angle for various times during injection of 500 ppm of ALFOTERRA S23-13S 90M	28
Table 5: Dynamic Water Advancing Contact Angle for various times during injection of 100 ppm of ALFOTERRA S23-13S 90.....	32
Table 6: Dynamic Water Advancing Contact Angle for various times during injection of 100 ppm of ALFOTERRA S23-11S 90 surfactant.	35
Table 7: Dynamic Water Advancing Contact Angle for various times during injection of 100 ppm of ALFOTERRA S23-9S 90.....	37
Table 8: Dynamic Water Advancing Contact Angle for various times during injection of 100 ppm of ALFOTERRA S23-7S 90 surfactant.	40
Table 9: Dynamic Water Advancing Contact Angle for various times during injection of 2000 ppm of SOLOTERRA 961 surfactant.....	47
Table 10: Dynamic Water Advancing Contact Angle for various times during injection of 2000 ppm of SOLOTERRA 939.....	48
Table 11: Dynamic Water Advancing Contact Angle for various times during injection of 2000 ppm of SOLOTERRA 970.....	50
Table 12: Dynamic Water Advancing Contact Angle for various times during injection of 2000 ppm of SOLOTERRA 938.....	52
Table 13: Quantitative drop dynamics and calculated bond numbers for the oil drop on the lower crystal during the injection of 100 ppm of Alfoterra 13S.....	57
Table 14: Quantitative drop dynamics and calculated bond numbers for the oil drop on the lower crystal during the injection of 100 ppm of Alfoterra 11S.....	58
Table 15: Quantitative drop dynamics and calculated bond numbers for the oil drop on the lower crystal during the injection of 100 ppm of Alfoterra 9S.....	59
Table 16: Quantitative drop dynamics and calculated bond numbers for the oil drop on the lower crystal during the injection of 100 ppm of Alfoterra 7S.....	60
Table 17: List of tested surfactants	64
Table 18: Summary of results	69

LIST OF FIGURES

Figure 1: Schematic description of the DDDC technique for measurement of dynamic water advancing contact angles. (Rao, 2002)	12
Figure 2: Structural representation of Alcohol Alkoxy	15
Figure 3: Structural representation of Alkyl Ether Carboxylate.....	15
Figure 4: Alcohol Propoxy Sulfate (Sasol).....	19
Figure 5: Alkyl Ether Carboxylates (Sasol).....	20
Figure 6: Ambient Optical Cell used in Contact Angle and IFT Measurements (Yu Zheng, 2012).....	20
Figure 7: (A) is a schematic presentation of the soxhlet system. Reprinted from Experimental organic chemistry: Principles and Practice, by L. M. Harwood and C. J. Moody. (B) is the actual soxhlet setup used and (C) are the unpolished crystals cut to the required dimension.....	22
Figure 8: Photographic depiction of dynamic contact angle movement of a Yates oil drop.....	23
Figure 9: Variation of Dynamic Contact Angle and TPCL movement with Time.....	25
Figure 10: Photographic depiction of Yates oil drop dynamic behavior during injection of 500 ppm of ALFOTERRA S23-7S 90 surfactant.	26
Figure 11: Variation of advancing dynamic contact angle with time during injection of 500 ppm of ALFORTERRA S23-7S 90M.....	27
Figure 12: Photographic depiction of Yates oil drop dynamic behavior during injection of 500 ppm of ALFOTERRA S23-13S 90 surfactant.	28
Figure 13: Variation of advancing dynamic contact angle with time during injection of 500 ppm of ALFOTERRA S23-13S 90M.	29
Figure 14: Photographic depiction of Yates oil drop dynamic behavior during injection of 100 ppm of ALFOTERRA S23-13S 90 surfactant.	31
Figure 15: Variation of advancing dynamic contact angle with time during injection of 100 ppm of ALFOTERRA S23-13S 90M	32
Figure 16: Variation of advancing dynamic contact angle with time during injection of 100 ppm of ALFOTERRA S23-11S 90.....	33
Figure 17: Photographic depiction of Yates oil drop dynamic behavior during injection of 100 ppm of ALFOTERRA S23-11S 90 surfactant.	34
Figure 18: Variation of advancing dynamic contact angle with time during injection of 100 ppm of ALFOTERRA S23-9S 90M.	36
Figure 19: Variation of advancing dynamic contact angle with time during injection of 100 ppm of ALFOTERRA S23-9S 90M.	38

Figure 20: Dynamic Water Advancing Contact Angle for various times during injection of 100 ppm of ALFOTERRA S23-7S 90 surfactant.	39
Figure 21: Variation of advancing dynamic contact angle with time during injection of 100 ppm of ALFOTERRA S23-7S 90M	40
Figure 22: Photographic depiction of Yates oil drop dynamic behavior during injection of 100 ppm of ALFOTERRA K3-41S surfactant.	40
Figure 23: Photographic depiction of Yates oil drop dynamic behavior during injection of 100 ppm of ALFOTERRA K45-DS surfactant.	41
Figure 24: Graphical presentation of IFT variation with time for ALFOTERRA 13S with pictorial depiction of the behavior of the crude oil sample at various instances during testing. ..	42
Figure 25: Graphical presentation of IFT variation with time for ALFOTERRA 11S with pictorial depiction of the behavior of the crude oil sample at various instances during testing. ..	43
Figure 26: Graphical presentation of IFT variation with time for ALFOTERRA 9S with pictorial depiction of the behavior of the crude oil sample at various instances during testing.	43
Figure 27: Graphical presentation of IFT variation with time for ALFOTERRA 7S with pictorial depiction of the behavior of the crude oil sample at various instances during testing.	44
Figure 28: Photographic depiction of Yates oil drop dynamic behavior during injection of 2000 ppm of SOLOTERRA 960 surfactant.	46
Figure 29: Photographic depiction of Yates oil drop dynamic behavior during injection of 2000 ppm of SOLOTERRA 961 surfactant.	46
Figure 30: Variation of advancing dynamic contact angle with time during injection of 2000 ppm of SOLOTERRA 961.....	47
Figure 31: Photographic depiction of Yates oil drop dynamic behavior during injection of 2000 ppm of SOLOTERRA 939 surfactant.	48
Figure 32: Variation of advancing dynamic contact angle with time during injection of 2000 ppm of SOLOTERRA 939.....	49
Figure 33: Photographic depiction of Yates oil drop dynamic behavior during injection of 100 ppm of SOLOTERRA 970 surfactant.	49
Figure 34: Variation of advancing dynamic contact angle with time during injection of 2000 ppm of SOLOTERRA 970.....	50
Figure 35: Photographic depiction of Yates oil drop dynamic behavior during injection of 2000 ppm of SOLOTERRA 938 surfactant.	51
Figure 36: Variation of advancing dynamic contact angle with time during injection of 2000ppmof SOLOTERRA 938.	52
Figure 37: Graphical presentation of IFT variation with time for SOLOTERRA 960 with pictorial depiction of the behavior of the crude oil sample at various instances during testing. ..	53

Figure 38: Graphical presentation of IFT variation with time for SOLOTERRA 961 with pictorial depiction of the behavior of the crude oil sample at various instances during testing. ..	53
Figure 39: Graphical presentation of IFT variation with time for SOLOTERRA 970 with pictorial depiction of the behavior of the crude oil sample at various instances during testing. ..	54
Figure 40: Graphical presentation of IFT variation with time for SOLOTERRA 938 with pictorial depiction of the behavior of the crude oil sample at various instances during testing. ..	54
Figure 41: Schematic presentation of the equilibrium drop between the two crystal surfaces (Ayirala et al., 2006)	56
Figure 42: Variation of drop dimensions with time for the drop on the lower crystal during injection of 100 ppm of Alfoterra 13S.....	57
Figure 43: Variation of bond numbers with time for the drop on the lower crystal during injection of 100 ppm of Alfoterra 13S.....	57
Figure 44: Variation of drop dimensions with time for the drop on the lower crystal during injection of 100 ppm of Alfoterra 11S.....	58
Figure 45: Variation of bond numbers with time for the drop on the lower crystal during injection of 100 ppm of Alfoterra 11S.....	58
Figure 46: Variation of drop dimensions with time for the drop on the lower crystal during injection of 100 ppm of Alfoterra 9S.....	57
Figure 47: Variation of bond numbers with time for the drop on the lower crystal during injection of 100 ppm of Alfoterra 9S.....	59
Figure 48: Variation of drop dimensions with time for the drop on the lower crystal during injection of 100 ppm of Alfoterra 7S.....	60
Figure 49: Variation of bond numbers with time for the drop on the lower crystal during injection of 100 ppm of Alfoterra 7S.....	60
Figure 50: Bond number comparative plot for Alfoterra 13S, 11S, 9S and 7S as a factor of time.	62
Figure 51: Duration of time for the initial Yates crude oil droplet to leave the lower crystal during injection of 100 ppm of the four ALFOTERRAs.....	65

ABSTRACT

Past studies of surfactants for enhanced oil recovery by wettability improvement, have often categorized surfactants as either non-ionic, anionic or cationic. This research has been done in an attempt to study different surfactants under the same group in greater detail by varying their structures and to classify them on the basis of their abilities to alter reservoir wettability. Two different families of surfactants, both anionic, namely alkyl alkoxy sulfates and alkyl ether carboxylates, have been studied. Surfactants tested in each of these groups are tuned individually by the level of hydrophobicity that they offer by varying the nature of the anionic head group and the number of ethylene oxide and propylene oxide units that are present in their chemical structures.

The experimental study is based on the Dual Drop Dual Crystal (DDDC) technique of dynamic contact angle measurement. Ten different surfactants, designed, manufactured and supplied by Sasol, were tested in a Yates oil – Limestone – Yates synthetic brine system at ambient conditions. The concentration levels of the surfactants were kept very low. This enabled a substantially increased reaction time for the system to interact with the surfactant. It also helped isolate the effect of interfacial tension reduction and study the wettability alteration, if any, with clarity. Interfacial tension measurements as a factor of time were also conducted to determine its effect over extended periods of time, as opposed to effects of wettability alteration of the system.

The surfactant structures were tested in order of decreasing hydrophobicity. Initial experimental results using reasonable concentration levels showed no varying effects between the individual surfactants. However upon considerable reduction of the surfactant concentration, each surfactant showed a variable effect on the oil droplet in terms of the measured

dynamic contact angle measured as well as a factor of time. The dimensionless Bond numbers calculated for these surfactants helped quantify the rock fluids interactions by taking into consideration both possible wettability alteration as well as the reduced interfacial tension. It was found that no two extremes of a surfactant in terms of hydrophobicity or hydrophilicity were ideal for the system. The challenge of trying to classify surfactants that are so similar in structure also made way for an alteration in the way results obtained from the DDDC technique are conventionally interpreted.

Surfactants have always been a popular choice in the field of enhanced oil recovery. However, no systematic means of classification yet exists that links the structure of a surfactant to its ability to alter reservoir wettability, especially when trying to classify surfactants that all belong to one singular family. This study is a step forward in that direction, to try and create a means of quantifying the effect that a particular structural variance could have on the potential recovery from a reservoir via altered wettability.

1. INTRODUCTION

Enhanced oil recovery has always been and will continue to be an essential part of the oil and gas industry. Surfactant flooding is one of the many EOR techniques that are employed to recover oil from depleted reservoirs. Surfactants aid in mobilizing the trapped oil in the porous media by significantly reducing the interfacial tension at the interface between the water/brine and oil and eventually forming microemulsions. However chemical flooding has always been an expensive process with marginal profits due to the adsorption of the surfactant by the reservoir rock. In recent times though, it has been discussed that adsorption by the porous media can aid in preferential wettability alteration which can in turn reap higher recoveries.

Over the years considerable research has been conducted on surfactants (Gupta et al., Solairaj et al., Seethapli et al., Hirasaki et al.). For the longest period of time, the oil and gas industry had its focus on sandstone reservoirs since they tend to have higher recoveries. Hence a lot of the surfactants researched upon and used were anionic surfactants. Beginning the mid 1980's, the focus started shifting to carbonate reservoirs and the effect of surfactants on them. By theory, a cationic surfactant would be an ideal choice for carbonate formations since they usually carry a positive surface charge which would result in less adsorption of the surfactant by the formation.

However, anionic surfactants have been found to be effective in yielding good recovery even in carbonate formations (Gupta et al., 2009). An aspect that is of particular importance here, is the wettability altering potential that anionic surfactants have displayed over the years in various studies (Somasundaran & Zhang, 2006, Hirasaki and Zhang, 2004, Seethapalli et al., 2004, Rao et al., 2006). A great deal of work has been done so as to compare the wettability alteration effects

of non-ionic, anionic and cationic surfactants in both sandstone and carbonate reservoirs (Anderson, 1986).

This study focuses on studying and comparing the different strains of surfactants that fall exclusively under the anionic family on a carbonate system and to try and compare the possible wettability alteration effects that they have on our system. Carbonate reservoirs in general may have low porosity and be fractured. In addition they usually exhibit an oil-wet nature (Manrique, Gurfinkel, & Muci, 2004). All of these properties make oil recovery from such formations relatively low. However studies have shown recoveries with surfactant flooding can be as high as 60% of the OOIP at very low surfactant concentrations and reservoir temperature conditions (Gupta & Mohanty, 2010). This recovery can be attributed due to both a reduction in interfacial tension as well as wettability alteration. The extent of such solid-liquid interfacial activity that alter surface charge and wettability are governed by the nature of the surfactants, minerals and solution conditions as well as reservoir rock chemistry (Somasundaran & Zhang, 2006).

Wettability alteration is directly related to surfactant adsorption. However, wettability changes are not only dictated by the amount of surfactant adsorbed but also by the structure and type of the surfactant adsorbed (Somasundaran & Zhang, 2006) as has been seen over the past in both literature and in the field. Seethapli et al., (2004) saw that propoxylated surfactants were capable of preferentially changing the reservoir wettability from oil-wet to water or intermediate-wet. Co-surfactants such as Sodium Carbonate, along with an anionic surfactant, help impart a negative zeta potential to the calcite/brine interface, which help promote water-wetness (Hirasaki & Zhang, 2004). Studies regarding the addition of propylene oxide or ethylene oxide to the surfactant molecule showed effects on the hydrophobicity and hydrophilicity of the surfactant which in turn affected its potential to alter the wettability of a system (Solairaj et al., 2013).

The system chosen by us as a base for this study is the West Texas Yates reservoir. Discovered in 1926, the Yates San Andres reservoir is a naturally fractured dolomite formation and has had a cumulative production over 1.3 billion barrels. San Andres is a 400 ft thick formation with average matrix porosity and permeability of 15% and 100md, respectively (Manrique, Gurfinkel, & Muci, 2004). It has been seen that chemical flooding in carbonate west Texas fields have resulted in significant amounts of oil recovery (Adams & Schievelbein, 1987). All of the surfactants tested have been injected into a system consisting of Yates crude oil, Yates synthetic brine and Limestone.

The objective of this study as stated earlier was on studying the effect that the structural changes in surfactants within the anionic family would have on its effectiveness in oil recovery via preferential wettability alteration. Measurement of the extent of such altered wettability can be done through numerous methods such as the Amott method, the USBM wettability index or by the measurement of water advancing contact angles amongst many others (Anderson 1986). For this study, our select group of surfactants, each belonging either to the group of Alkyl Alkoxy Sulfates or Alkyl Ether Carboxylates were tested via the dual drop dual crystal (DDDC) technique of contact angle measurement (D. N. Rao & Girard, 1996).

2. LITERATURE REVIEW

Surfactants have been an integral part of the oil and gas industry and it continues to be of significance even today. They find various applications at all levels right from drilling to production and reservoir injection (Schramm, 2000). Surfactant injection form a part of chemical flooding and fall under the subsidiary of enhanced oil recovery or EOR. Surfactants are injected solely by themselves but more often in combination with a polymer or an alkaline or both and are popularly known as SP (surfactant-polymer) or ASP (alkaline surfactant polymer) floods.

Since oil and water don't mix, there exists a high interfacial tension between the two phases. As a result oil does not tend to flow easily through the pores in the reservoir rock. Surfactants are hence used to reduce this interfacial tension to ultra-low levels, thereby reducing the capillary pressure and causing mobilization of the oil phase (Arabia & Box, 2011). Surfactants have also have been seen to at times preferentially alter the wettability of the reservoir which aids improved recovery. However the type of surfactant used for any flood is dependent on parameters such as the reservoir rock type, brine salinity and temperature conditions (Morrow, 1990). Each of these parameters decide the nature of the surfactant used so as to get the required IFT reduction, possible wettability modification, desirable phase behavior effects and minimized adsorbtion. This chapter is an overview of the structure and mechanisms associated with surfactants, their classification and also a background of the history and type of surfactants used in the industry, with special focus on the structural effects of surfactants belonging, in particular, to the anionic family.

2.1 Surfactant Structure, Type and Micelle formation

Surfactants are organic compounds that are amphiphilic. That is, they have a hydrophobic tail group and a hydrophilic head group attached to it. These molecules form layers at an interface

and show surface activity due to the strong interactions that the polar head group has with its aqueous environment. They are usually classified by the hydrophilic head group that it bears and can be either anionic (negative), cationic (positive), amphoteric (charge is dependent on pH), zwitterionic (both positive and negative charges) or nonionic (no charge) (Schramm, 2000). The interfacial properties of the surfactant can be tailored by altering the tail group in terms of length or branching.

At extremely low concentration levels, surfactants behave simply as a normal electrolyte. However as the concentration is increased surfactant molecules spontaneously aggregate in what is known as micelle formation. This phenomenon happens only at and above a specific concentration level known as the critical micelle concentration or CMC. The hydrophobic tail group of the surfactant associate on the interior while the polar heads are on the outside since they react more strongly with the aqueous environment. Hence it forms a hydrophilic outer layer that prevents the oil droplets, that is the hydrophobic heads, from merging into larger droplets (Schramm, 2000).

In most EOR processes involving surfactants the surfactant must usually be present at or higher than the CMC value since its greatest effect, such as lowering of interfacial tension, is seen when there is a significant concentration of micelles (Sasol, n.d.-c). The CMC value also denotes the point of maximum surface adsorption of the surfactant onto its surrounding, however there is very little adsorption increase at a point beyond the CMC (Schramm, 2000). It is worth mentioning at this point that a lot of the experimental runs made as part of this research, employed surfactants at concentration levels as low as 100 ppm (ALFOTERRAs) but were significantly above the CMC levels for each of the respective surfactants.

2.2 Effect of Surfactants on Interfacial Tension

Surfactants are used in combination with water-floods or ASP floods so as to reduce the amount of external mechanical energy required to overcome the interfacial tension so as to make the oil flow through porous rocks. Surfactant molecules are adsorbed at the interface and provide an expanding force against the existing contracting force or interfacial tension thereby causing an IFT reduction. This can be seen numerically in Young-Laplace's equation for capillary pressure 'Pc'.

$$P_c = \frac{2\gamma\cos\theta}{R} \quad (1)$$

The interfacial tension between the phases causes an imbalance in the pressure across the curved surface with the greatest pressure being inside the bubble. Therefore

$$P_c = p_A - p_B \quad (2)$$

A and B denote the two phases. Liquid flow due to this pressure difference is known as capillary flow. A reduction in IFT automatically reduces the capillary pressure which is directly related to oil recovery and has been discussed in the following sections (Schramm, 2000). To achieve low values of residual oil saturation, the IFT needs to be reduced from 20-30 N/mm to values in the range of 0.001 to 0.01 mN/m. (Hirasaki, Miller, & Puerto, 2011). Several surfactants such as petroleum sulfonates have been seen to yield such ultra-low interfacial tension values at concentrations less than 1 percent by weight (Hill, Reisberg, & Stegemeier, 1973).

The most popular methods to measure interfacial tension are by using the sessile drop or pendant drop techniques. However the spinning drop technique is by far the most suitable for measuring ultra-low IFT at reasonably high temperatures. In our case, even though the measurements have been done at ambient conditions, the spinning drop technique has been

adopted since we aimed at acquiring the interfacial tension values as a fraction of time and the spinning drop technique was the easier and more suitable of all the other methods for this purpose.

2.3 Structural Effects of Surfactant on Interfacial Tension

Over the years surfactant structures have been modified to help achieve ultra-low interfacial tension. Reduction of the interfacial tension results in the formation of microemulsions and solubilization (Sasol, n.d.-c). The formation of a desirable microemulsion is extremely important for maximizing oil recovery. Type III Winsor phase is considered as the most desirable microemulsion since it exhibits the lowest interfacial tension (Duscha, Boukari, & Shcherbakov, 2014). A lot of surfactants in the past used alcohol as a co-solvent to prevent the formation of undesirable viscous phases and emulsions instead of the desired low-viscosity microemulsions (Hirasaki et al., 2011). This is because long linear chain surfactants tend to form viscous phases (Levitt, 2006). Using surfactants with branched hydrocarbon chains and adding ethylene oxide (EO) and/or less-hydrophilic propylene oxide (PO) groups to the surfactant, as well as using mixtures of surfactants with different hydrocarbon-chain lengths or structures reduce or eliminate the possibility of such undesirable microemulsions at temperatures below 60°C (Hirasaki et al., 2011).

Brine salinity is another factor which affects the interfacial activity of a surfactant. This is again because salinity dictates phase behavior and the kind of microemulsion formed (Duscha et al., 2014). It is for this reason that in addition to the original surfactant, co-surfactants such as NaCl are very commonly used in combination to help meet the salinity requirements so as to achieve the lowest interfacial tension (Nelson, Lawson, Thigpen, & Stegemeier, 1984). In the case of petroleum sulfonate surfactants, optimum concentrations of NaCl helped achieve IFT values as low as 10^{-4} mN/m (Hill et al., 1973). In addition, surfactants are also affected by the presence of

different ions in the reservoir brine. For example, anionic surfactants in general are sensitive to multivalent cations such as magnesium, barium and calcium and each of these are ions are present in most reservoir brines. However, a co-surfactant such as NaCl helps conserve the interfacial activity of the anionic surfactant. As much as 500 ppm of calcium ion can be tolerated in 0.1 molar NaCl at elevated temperatures (Hill et al., 1973). Alcohols can also act as co-surfactants. Alcohols with short chains increase optimal salinity for sulfonate surfactants, while longer-chain alcohols decrease optimal salinity. (Hirasaki et al., 2011).

However Maerker & Gale, 1992 found that optimal salinity requirements, and in turn significant IFT reduction, could also be met with the introduction of EO/PO units in the surfactant structure and not using a co-surfactant at times. Optimal salinity increases with more ethoxyl groups and decreases with more propoxyl groups. Weakly hydrophobic functional groups such as propylene oxide (PO) also have the added benefit of increasing the breadth of the ultralow IFT region (Duscha et al., 2014).

It should be noted that the addition of PO/EO units also have an effect on equivalent alkane carbon number (EACN) of the oil. It was seen that as the oil EACN increased, the hydrophobe size required to achieve ultra-low IFT increased (Solairaj et al., 2013). But the molecular weight of the surfactant also poses a limitation. Hill et al., 1973, evaluated aqueous surfactant systems using petroleum sulfonates and it was seen that neither low nor high molecular weight commercial sulfonates were as effective at yielding higher levels of interfacial activity as mixtures of low and high molecular-weight sulfonates, with an average molecular weight of 410 to 450.

Therefore it can be concluded that addition of propylene oxide to the surfactant not only improves its performance but is also cost effective and a very practical approach to tailoring the

surfactant to the specific crude oil and reservoir conditions for both sandstone and carbonate reservoirs (Duscha et al., 2014).

2.4 Wettability Alteration and Contact Angle Measurement

Wettability is the tendency of one fluid to spread on or adhere to a solid surface in presence of other immiscible fluids (Anderson, 1986). Wettability is extremely important from a petroleum aspect because the preferential wetting nature of a reservoir can either assist or interfere with oil recovery. This aspect is of even higher significance during EOR processes such as ASP floods.

Both adsorption and wettability changes are influenced mainly by the chemical structure and mix of the surfactants. Surface chemistry of the rock, oil and brine compositions, nature of the polymers added and solution conditions such as salinity, pH and temperature also play a pivotal role (Somasundaran & Zhang, 2006). Over the years numerous methods have been discussed to try and alter the wettability to preferentially water wet. Hirasaki and Zhang (2004), discussed that in using an alkali, Sodium Carbonate, along with an anionic surfactant, would help impart a negative zeta potential to the calcite/brine interface, thereby trying to replicate surface charge conditions of a sandstone reservoir, which was believed to promote water-wetness. Gupta et al., (2009) screened anionic and non-ionic surfactants and identified change in contact angle of an initially oil-wet calcite plate for all possible types of reservoirs conditions, namely low temperature-low salinity, high temperature-low salinity, low temperature-high salinity and high temperature-high salinity. Chen et al., (2000) conducted imbibition tests on oil wet Yates reservoir system and found that the recovery increased by 40% by static imbibition of dilute surfactants as compared to just water imbibition. They concluded that the increase in recovery was a contribution of both reduced IFT as well as preferential wettability alteration.

Anderson (1986) discussed the various ways that wettability could be measured. The Amott method, contact angles measurements or the USBM wettability index are some of the existing quantitative methods while qualitatively, the imbibition method, microscope examination, floatation methods, glass slide method or the relative permeability method exist. The method of defining wettability by contact angle has been considered to be the most direct. It has been defined as the most universal measure of the wettability of surfaces (Morrow, 1990). This experimental technique is based on the fact that the water wetting process is an oil displacement phenomenon on the solid surface (Somasundaran & Zhang, 2006) which is a measure of the true water advancing angle.

A variety of techniques exist for the measurement of this contact angle such as the static sessile drop method, pendant drop method, dynamic sessile drop method, Wilhelmy's method and Washburn's equation capillary rise method. In terms of contact angles, the range from 0 to 60 degrees is considered to be a strongly water wet system, 60 to 120 degrees range is considered to be a system having intermediate wettability while angles ranging from 120 to 180 degrees indicate a strongly oil wet nature. The contact angle plays a significant role in oil recovery via capillary pressure

Water wet reservoirs are usually the ones with better recoveries compared to oil wet reservoirs. However even at its best, the total oil recovered during primary recovery as well as a water-flood is usually at about 30% of the OOIP. The rest of the oil is trapped in the smaller pores of the reservoir where the driving viscous force of the water-flood couldn't overcome the capillary pressure to drive the oil out. It is here that surfactants play a major role. The capillary number helps give us a better understanding of the role of a surfactant. In general, the ratio of the viscous forces to the capillary forces is defined as the capillary number N_c .

$$N_c = \frac{\text{Viscous forces}}{\text{Capillary forces}} = \frac{\eta v}{\gamma \phi} \quad (3)$$

η is the velocity and v is the viscosity. γ is the interfacial tension and ϕ is the porosity. The velocity and viscosity can be increased to overcome the capillary forces but there are always mechanical restrictions to the size and horsepower of a pump. However, if surfactant were to be added to the water-flood, it would result in a lower IFT value thereby reducing the existing capillary pressure for movement of the trapped oil.

In 1994, Rao and Girard introduced a new techniques for dynamic contact angle measurement known as the dual drop dual crystal technique or the DDDC technique wherein individual oil droplets were placed on two polished crystals made from the requisite reservoir rock type placed in an environment of reservoir/synthetic brine and aged. Eventually the bottom crystal is flipped and the oil droplets are merged and let to age yet again. The contact angle measurements are made by making gradual shift on the lower crystal only and the angle that the droplet makes at the point of movement initiation on the crystal in the water phase is measured as the water advancing angle. The three phase contact line or the TPCL movement is also monitored since it is what defines an advancing angle. A water-wet case, intermediate-wet case and oil-wet case were demonstrated. (D. N. Rao & Girard, 1996)

In 1996, Rao discussed the concept and definition of advancing and receding contact angles as well as introduced a new technique of measuring them at elevated temperatures and pressure using the dual drop dual crystal technique. He questioned as to if water receding angles were a better definition for stating the native wettability of the system since it is oil that migrates and displaces the oil in a reservoir. However since water-flooding involves the expulsion of oil from the reservoir by water, water advancing contact angles have a more conforming definition for the wettability of a system. (Rao, 2002)

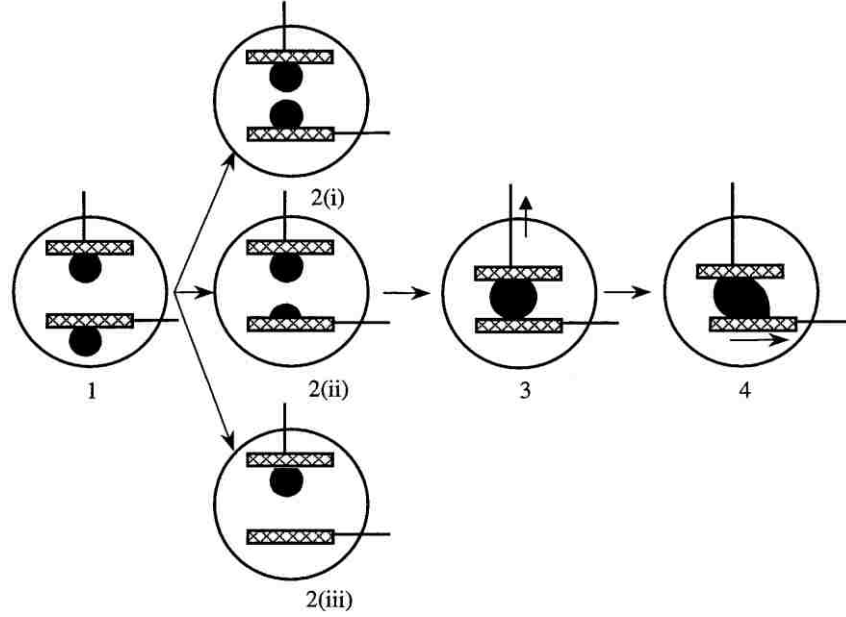


Figure 1: Schematic description of the DDDC technique for measurement of dynamic water advancing contact angles. (Rao, 2002)

Ayirala et al., 2006 investigated a new procedure to simulate the process of wettability alteration in a fractured reservoir due to surfactant flooding. These alterations were defined by the dimensionless Bond number. For the purpose of analyzing the effects of surfactant injection, the Bond number was redefined as

$$N_B = \frac{\Delta\rho g(h - h_i)d}{\sigma \cos\theta} \quad (4)$$

Where, N_B is the bond number, $\Delta\rho$ is the density difference in gm/cc, σ is the interfacial tension in mN/m, h_i is the initial height of the drop in equilibrium at $t=0$, d is the drop diameter and h is the height of the drop on the lower crystal at a given time t . Bond numbers help give an overview of the effect of the surfactant on the enhanced oil recovery since it takes into consideration both the interfacial tension reduction as well as possible wettability alteration in terms of the contact angle

measured. It was found that anionic surfactants were more effective in altering the wettability than a non-ionic surfactant. (Ayirala, Vijapurapu, & Rao, 2006)

2.5 Structural Effects of Surfactants on Wettability-

Just as the structure of a surfactant affects its interfacial activity, the same holds true in the case of its potential to change wettability of a reservoir. Over the years, surfactants have been tailored and optimized to alter the wettability preferentially to water-wet since water wetness promotes greater recovery (Hirasaki et al., 2003). One of the major structural additions have been the introduction of PO and EO units into the surfactant chain. The reason ethoxylated and propoxylated sulfate surfactants have been investigated so much is due to their tolerance to divalent ions present in reservoir brines (Hirasaki & Zhang, 2004) but they have also been seen to influence wettability.

Seethapalli et al., (2004) conducted experiments with anionic surfactants belonging to the Alfoterra class which were propoxylated sulfates and found that the most of the samples (Alfoterra – 35, 38, 63, 65, 68) belonging to this class changed the wettability from oil wet to intermediate or water wet. One of the problems faced by the propoxylated sulfates is the temperature restriction. This is because at elevated temperatures, sulfate hydrolysis occurs (Hirasaki & Zhang, 2004). Gupta et al., 2009 screened surfactants based on temperature, salinity, hardness and conducted subsequent wettability studies. The Alfoterra 38, 35 and 68 (propoxy sulfate) performed well at room temperature at around 25° C but precipitated out at higher temperatures of 90° C. It was found that ethoxylation (addition of EO units) stabilized the surfactants at higher temperatures. The screened surfactants were observed to have the same optimal salinity for both IFT and contact angle measurements for a given surfactant concentration with different oils. The extent of wettability alteration decreases with increase in salinity. Hence the surfactants screened could be

used in low salinity conditions or in the presence of a co-surfactant that controls the salinity in high salinity reservoirs.

However Rao et al., (2006) studied the impact of low cost surfactants on wettability and results showed that the anionic ethoxy sulfate surfactant used, resulted in reverse wettability alteration on the Yates reservoir system, wherein the system became even more oil wet. Gradual decrements in oil recoveries were due to the strongly oil-wet state induced by the surfactant.

Therefore it is imperative to realize that the introduction of PO and EO units have to be tailored specific to a particular system. However, a variety of surfactants used by the industry are broadly classified under distinct categories. The ones pertinent to this study are surfactants belonging to the commercial line of Alfoterras and Soloterras. Both line of surfactants are manufactured by the company Sasol, each designed for different reservoir conditions. The ALFOTERRA or Alcohol Alkoxy Sulfates are based on different feed alcohols with varying PO/EO units and have (Sasol, n.d.-a; Sasol, n.d.-b):

- Good salinity tolerance
- Low critical microemulsion concentration c_{mc})
- Hydrophobic tail can be made from a variety of different chain length branched, semi-branched, or linear alcohols
- Optimum temperature and salinity adjustable by hydrophobe and PO/EO grade
- Can form microemulsion without aid of a cosurfactant/cosolvent
- Compatible with alkali to reduce interfacial tension and enhance phase behaviour
- Usualy used for reservoir conditions below a maximum temperature of $\sim 60^{\circ}\text{C}$

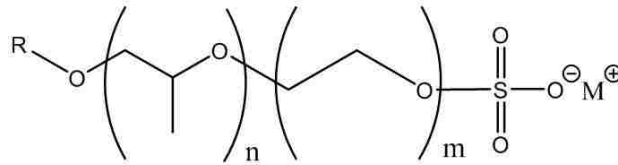


Figure 2: Structural representation of Alcohol Alkoxy

The other commercial line of surfactants are the Alcohol Ether Carboxylates and they belong to the family of Soloterras. They are relatively new to the industry and are available based on different feed alcohols as well as different alkoxylation grades and have (Sasol, n.d.-a; Sasol, n.d.-b):

- Typically a high salinity surfactant but optimum is adjustable by hydrophobe and PO/EO grade and by the addition of a co-surfactant.
- Excellent salinity tolerance
- Used as a primary surfactant but at times also used as a co-surfactant
- Good temperature stability

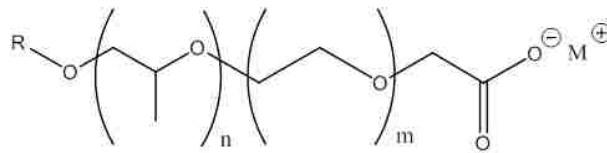


Figure 3: Structural representation of Alkyl Ether Carboxylate

In 2015 Jürgenson, G Alvarez et al., published a paper on similar alkyl ether carboxylates as a novel surfactant for enhanced oil recovery. Alkyl ether sulfates perform well in a high salinity environment but are thermally stable to only about 60 C (Adkins et al., 2010). The only exception to this is if they are used at an elevated pH of 10-11 by using an alkali. However an alkali cannot

be always used. To overcome the thermal barrier, the surfactant's hydrophilic head group was modified and a carboxylate functional group was introduced to form alkyl ether carboxylate. They concluded that the surfactant was chemically stable beyond 60 °C as well as in high salinity conditions. Therefore it was considered a viable candidate for EOR for a large range of reservoirs. (Jürgenson, Bittner, Oetter, Se, & Corp, 2015)

The overall effect of PO and EO units was investigated by Solairaj et al., (2013). He published a new correlation that took into account the effect of the propylene oxide number (PON), ethylene oxide number (EON), temperature, brine, salinity and the equivalent alkane carbon number (EACN) of the oil. It was seen that as the oil EACN increased, the hydrophobe size required to achieve ultra-low IFT increased. This is one of the main reasons for the need of large hydrophobe surfactants, i.e. a longer tail. However, just the EACN is not the sole contributor towards the hydrophobicity of a surfactant and the presence of EO and PO units had a significant effect along with temperature. It was seen that larger hydrophobes are needed with an increase in temperature since the hydrophilic head of the surfactant interacts more strongly with water as temperature increases when it has an anionic head such as a sulfate or sulfonate. Also, some other important observations were that PO units were more hydrophobic than the EO units. The effect of each was not linear and most importantly, the EO and PO units had a more significant effect on the hydrophobicity when part of a smaller alkane chain such as C13 alcohol propoxylated sulfates or alcohol ethoxylated nonionic surfactants when compared to a longer one. (Solairaj et al., 2013)

Another structural variable that is of importance are sulfonates and sulfates as the hydrophilic head group. Sulfonates are more stable than sulfates at high temperatures. This is because the sulfur atom in sulfonates is attached to a carbon atom which is thermally more stable than the sulfur oxygen bond that exists in sulfates (Gupta, Mohan, & Mohanty, 2009). However

sulfates instead of sulfonates are preferred at lower temperatures because of the ease of availability (Hirasaki & Zhang, 2004).

3. EXPERIMENTAL APPARATUS AND MATERIALS

3.1 Materials

3.1.1 Rocks

The system used for testing of the surfactants was based off the Yates reservoir in West Texas which is known to be an oil wet reservoir (Wei et al., 2006) with dolomite constituting as its primary mineralogy. However the extremely oil wet nature between Yates oil and dolomite resulted in a hindrance in reproducibility with respect to measurement of contact angles. Hence, keeping in mind the requirement of an oil wet system and a carbonate rock, Limestone was chosen as our rock for the system. Limestone and Yates oil still form an extremely oil wet system but relatively less strongly oil wet when compared to the Dolomite and Yates oil system. The Limestone crystals were ordered from Ward's Nature Science.

3.1.2 Fluids and Chemicals

The fluids used in the system was Yates synthetic brine and Yates crude oil. The composition of the synthetic brine is given in the following table. The various salts were added to deionized water, stirred and then filtered and deaerated by a vacuum pump.

Table 1: Composition of Yates synthetic brine.

Salt	Chemical Name	Yates Brine (g/l)
NaCl	Sodium Chloride	2.546
KCL	Potassium Chloride	0.0915
Na ₂ CO ₃	Sodium Carbonate	1.43
CaCl ₂ .2H ₂ O	Calcium Chloride Dihydrate	1.555
MgCl ₂	Magnesium Chloride	1.87
Na ₂ SO ₄	Sodium Sulfate	2.2
NaHCO ₃	Sodium Bicarbonate	1.09
TDS		10.7825

3.1.3 Surfactants

A total of 12 surfactants were tested. All were anionic by nature but belonged to two different sub-families. The first group of surfactants were alcohol propoxy sulfates. Five different types were part of this study. Each one varied from the other by the number of propylene oxide units in them so as to change their level of hydrophobicity. These surfactants are in general suitable for low temperature environments and moderate to high salinity. They were supplied by Sasol under the trade name ALFOTERRA (Sasol Olefins & Surfactants, Lake Charles: Sasol). The surfactants tested were:

- ALFOTERRA G16-20S M
- ALFOTERRA® S23-13S 90
- ALFOTERRA® S23-11S 90
- ALFOTERRA® S23-9S 90
- ALFOTERRA® S23-7S 90
- ALFOTERRA K3-41S
- ALFOTERRA K45-DS

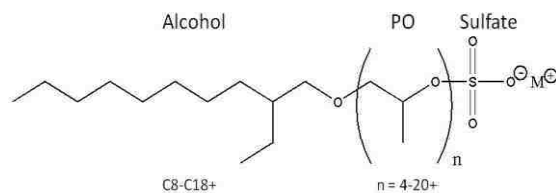


Figure 4: Alcohol Propoxy Sulfate (Sasol)

The second group were alkyl ether carboxylates. They usually have a combination of ethylene oxide and propylene oxide units. They are stable at high temperatures but limited to lower salinity levels. They are at times used in conjunction with a co-surfactant to stabilize it in higher salinity environments. They were also supplied by Sasol under the trade name SOLOTERRA (Sasol Olefins & Surfactants, Lake Charles: Sasol).

The surfactants tested were:

- SOLOTERRA 960
- SOLOTERRA 961
- SOLOTERRA 939
- SOLOTERRA 970
- SOLOTERRA 938

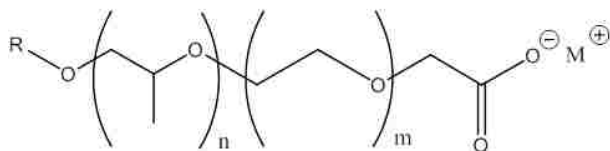


Figure 5: Alkyl Ether Carboxylates (Sasol)

3.2 Experimental Apparatus

3.2.1 DDDC Ambient Cell

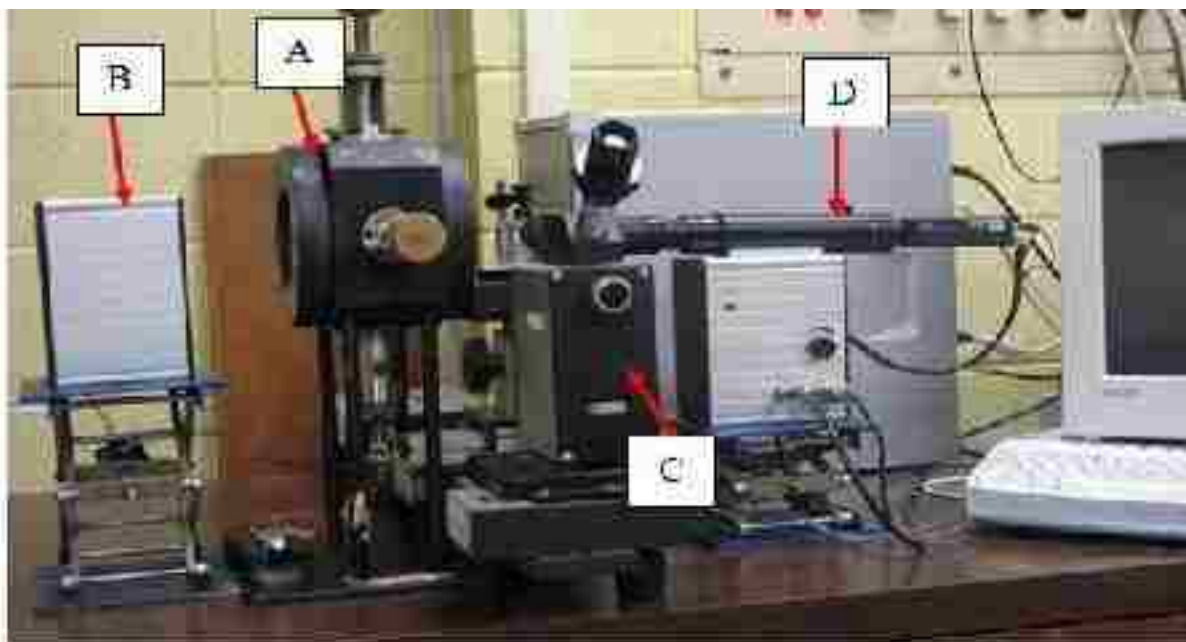


Figure 6: Ambient Optical Cell used in Contact Angle and IFT Measurements (Yu Zheng, 2012)

The experimental setup is based on the Dual Drop Dual Crystal (DDDC) technique of measuring dynamic contact angles. All measurements made on this apparatus are at ambient

temperature and pressure conditions. The setup consists of a cell with two rock crystal holders, one at the top and the other at the side. The holder at the top moves in the vertical direction while the holder on the side can move in the horizontal direction. Both holders are also free to rotate in their respective axes.

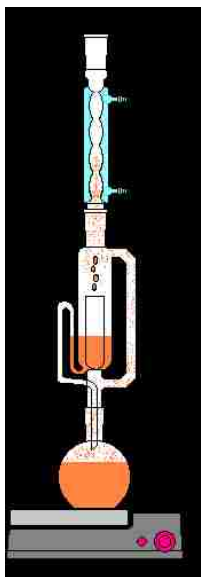
The bottom of the cell has a needle tip which is connected to a syringe for injecting oil into the cell. Two exit valves are located in the cell. One at the top and the other at the bottom. The cell is usually filled with brine. There is a halogen light source behind the cell and a camera located in front of the cell. The visuals captured by the camera are displayed on the computer connected to it. The various parts of our system are namely:

- A. Ambient cell
- B. Light source
- C. Goniometer
- D. Camera

3.2.2 Rock cutting and Soxhlet cleaning system

Each of the rocks are first cut into the form of a tile by means of an in-house cutter. The crystal for the holder on top is cut to the dimension of 0.4''x 0.5''x 0.2'' while crystal for the holder on the side is cut to the dimensions of 0.4''x 0.5''x 0.2''. Following this, the tiles were polished by three different polishing papers of different grit size.

The crystals are eventually cleaned in the Soxhlet system by using an organic solvent which is a mixture of 83% Methyl Alcohol and 17% Chloroform. It is treated to the solvent for a period of 24 hours. Subsequently, the crystals are boiled in deionized water for 2 hours and dried in an oven close to room temperature.



A



B



C

Figure 7: (A) is a schematic presentation of the soxhlet system. Reprinted from *Experimental organic chemistry: Principles and Practice*, by L. M. Harwood and C. J. Moody. (B) is the actual soxhlet setup used and (C) are the unpolished crystals cut to the required dimension.

4. RESULTS AND DISCUSSION

4.1 Wettability determination of Yates oil-Yates brine-limestone system at ambient condition.

For the purpose of measurement of dynamic contact angles, two polished crystals are introduced into a system containing the synthetic brine by means of two holders, one at the top and the other at the side. A single drop of the crude oil is then placed on both the top and bottom crystals and let to age for 24 hrs. The lower crystal is then flipped and both the drops are merged. The system is then again allowed to age for 5 hrs. Following this, the lower crystal is made to slide by either screwing it in or out via the holder. The drop between the two crystals is allowed to age for 90 min after each shift in position of the lower crystal. Figure 8 represents the photographic sequence for each position.

For each shift, the water advancing contact angle is measured. The three-phase contact line (TPCL) movement was also recorded at every stage. The TPCL was normalized by the distance between the lower left corner of the Yates oil drop and lower right edge of the crystal divided by the measured initial contact line position, R_i .

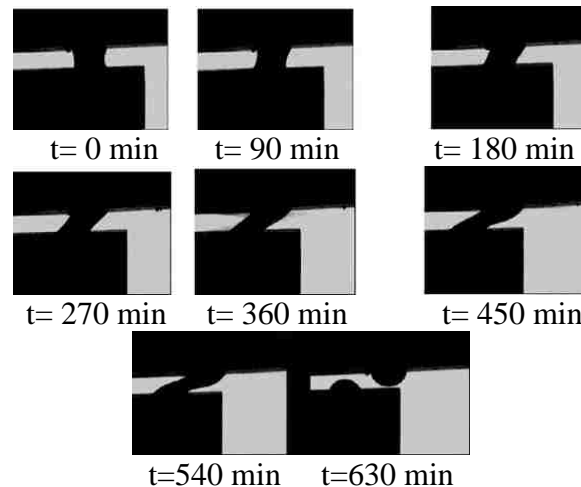


Figure 8: Photographic depiction of dynamic contact angle movement of a Yates oil drop

Table 2: Dynamic Water Advancing Contact angle as measured for initial system

Time	Θ_a	Left	Right	TPCL
0	122	338	179	1.888268
90	130	338	179	1.888268
180	129	338	179	1.888268
270	135	338	179	1.888268
360	148	338	179	1.888268
540	136	336	170	1.877095
630	138	336	170	1.877095

The contact angles and TPCL movements are plotted against time in Figure 9. The initial contact angle was 122° . It increased to a 130° on the first shift of the lower crystal at 90 minutes and kept increasing to reach a peak of 145° at 360 min. Up until this point there was no TPCL movement. However, at 540 min, the contact angle reduced to 136° . The observation to be noted at this point is that there was a slight shift in the TPCL. This implies that there was water encroachment onto a previously oil occupied area signifying that the contact angle of 148° measured at 360 min represents the water advancing contact angle for this system as there was no further movement in the TPCL at the subsequent shifts made at 540 min and 630 min.

At 630 min, a strongly adhering Yates oil drop, as seen in the last image of Figure 2, was left on the lower crystal surface. This was due to the fact that the adhesion force between the rock and the oil was more than the cohesive force in the oil drop held between the two crystals. The measured peak water advancing contact angle of 145° demonstrates that this system is strongly oil-wet at ambient conditions.

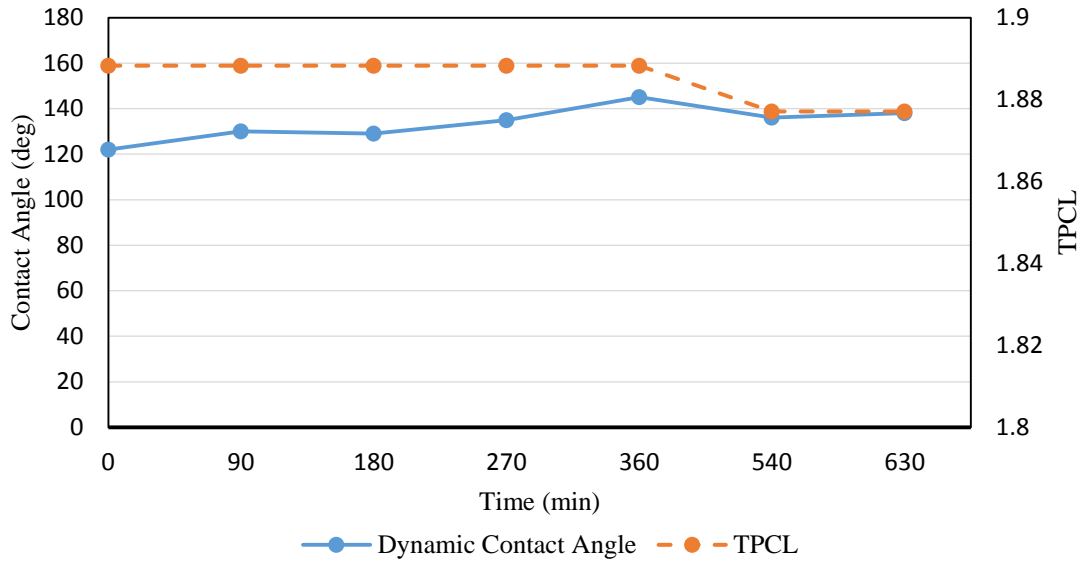


Figure 9: Variation of Dynamic Contact Angle and TPCL movement with Time

4.2 Initial Trials

Three different surfactants were injected into the system discussed above.

- ALFOTERRA S23 - 7S 90M
- ALFOTERRA S23-13S 90M
- SOLOTERRA 960

4.2.1 Injection of 500 ppm of ALFOTERRA S23-7S 90

Figure 10 is the photographic depiction of the injection of 500 ppm of ALFOTERRA S23-7S 90 of. It was seen that the drop floated away from the lower crystal onto to the top crystal in the first 40 seconds (i.e. from $t=0s$ to $t=40s$) leaving behind a small portion of the oil droplet. The lower left contact angle varied with time as shown in Figure 10 and fluctuated at around 138° with the peak at 147° which is the water advancing angle for this system due to the TPCL movement as seen from the video. Therefore the system remained oil wet.

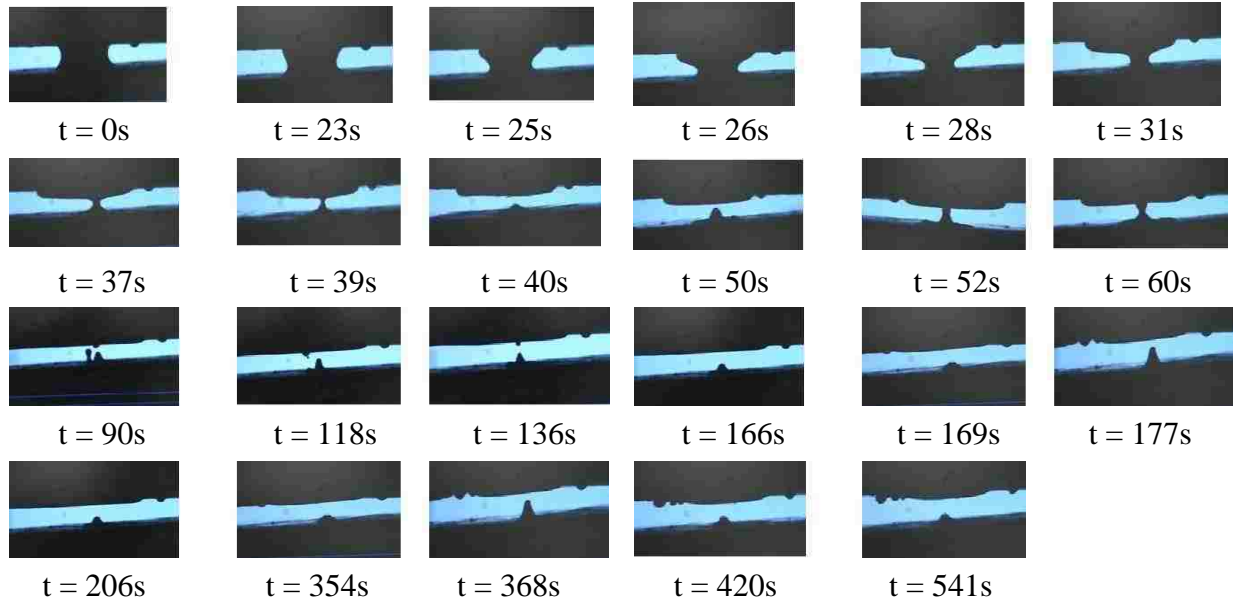


Figure 10: Photographic depiction of Yates oil drop dynamic behavior during injection of 500 ppm of ALFOTERRA S23-7S 90 surfactant.

Table 3: Dynamic Water Advancing Contact Angle for various times during injection of 500 ppm of ALFOTERRA S23-7S 90M.

Time (sec)	Θ_a (deg)
0	133
23	138
25	135
26	134
28	139
31	129
37	139
39	147
40	
50	127
52	134
60	135

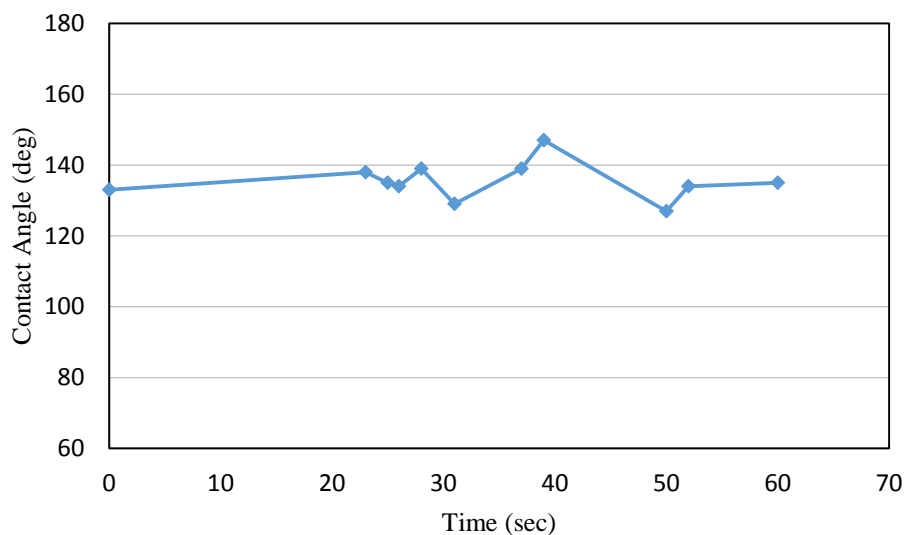


Figure 11: Variation of advancing dynamic contact angle with time during injection of 500 ppm of ALFORTERRA S23-7S 90M.

Further analysis was done on the residual oil that was left behind on the lower crystal. With further surfactant injection, the droplet began to move again at $t=50s$ and escaped to the upper crystal. This can be attributed to a combination of continued decrease in the interfacial tension and also surfactant adsorption onto the crystal face. The interaction of the surfactant with the crystal surface appears to be the cause of the droplet movement and the adhesion force between the oil and the crystal surface is the reason for the droplet to continue to adhere to the lower crystal.

At 118 seconds, there is again movement in the drop. However the drop separates into two smaller droplets. At 354 seconds, there is again a repeat formation of a smaller drop with an advancing contact angle of 137° which reduces to 130° at 368 seconds. Hence it can be seen that even over extended period of time, the dynamic water advancing angle is 137° which is not too different from the earlier measurements during surfactant injection.

When compared to the original system (with 148° advancing contact angle) with no surfactant injection, it can be observed that this surfactant had a very slight effect, if any, on the wettability in terms of reducing the measured water advancing contact angle to 137° .

4.2.2 Injection of 500 ppm of ALFOTERRA S23-13S 90M

Figure 12 is the photographic depiction of the injection of 500 ppm of ALFOTERRA S23-13S 90 surfactant into our system. In this case, as we can see the drop floated away from the lower crystal onto to the top crystal in the first 165 seconds (i.e. from t=0s to t=40s) leaving behind a small portion of the oil droplet. The bottom left contact angle varied with time as shown in Table 4 and fluctuated with a peak at 155°. This shows that the wettability of the system remained oil wet. Unlike case 4.2.1, there was no subsequent small drop formation on the lower crystal.

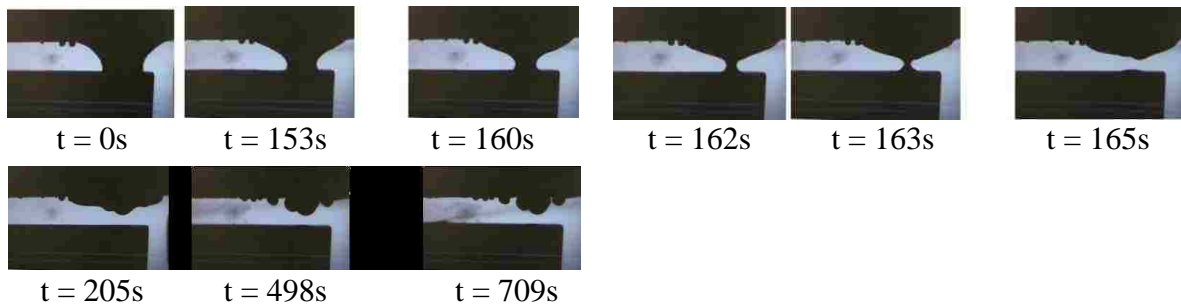


Figure 12: Photographic depiction of Yates oil drop dynamic behavior during injection of 500 ppm of ALFOTERRA S23-13S 90 surfactant.

Table 4: Dynamic Water Advancing Contact Angle for various times during injection of 500 ppm of ALFOTERRA S23-13S 90M

Time (sec)	Θ_a (deg)
0	136
153	135
160	133
162	155
163	150

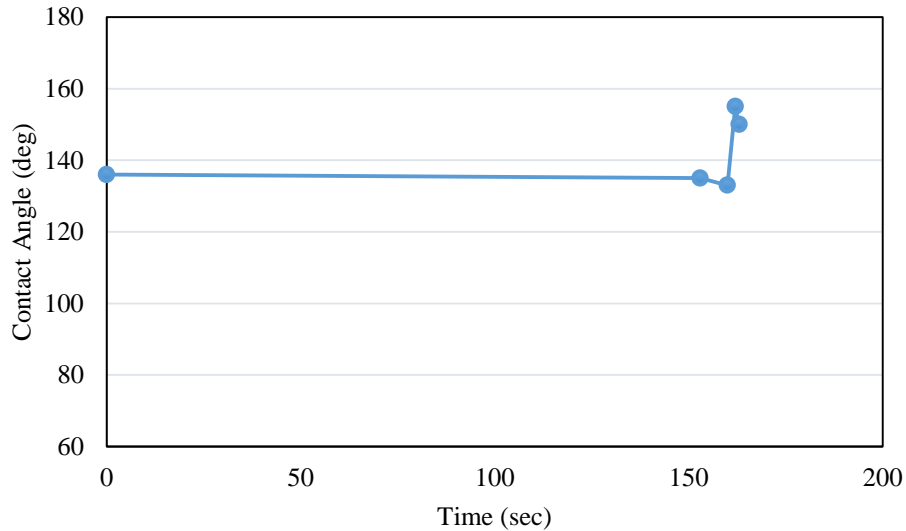


Figure 13: Variation of advancing dynamic contact angle with time during injection of 500 ppm of ALFOTERRA S23-13S 90M.

4.2.3 Injection of 1000 ppm of SOLOTERRA 960

For the injection of SOLOTERRA 960, the initial concentration used was 500 ppm. However there was no effect on the system with respect to contact angle. The drop remained stagnant in its position. A stronger concentration of 1000 ppm was injected. However, it yielded the same result. There was no change in the system even after an extended time of approximately 20 hours.

4.2.4 Conclusion from initial trials

As seen from the initial runs, the surfactants tested at a concentration of 500 ppm had very small reaction time with the max registered at 420 seconds and very little change in wettability was observed. In order to provide more reaction time, the surfactant concentration was lowered from 500 ppm to 100 ppm so as to extend the duration of experimental observations to about 8 hours. Two pore volumes (with respect to the cell) of the surfactant was introduced into the system so as to make sure that all of the initial brine was flushed and the surfactants were introduced into the system at an average rate of 11cc/min.

4.3 Effect of injection of Alkyl-Alkoxy Sulfates (ALFOTERRA) at a concentration of 100ppm

Over the next few sections of this chapter, namely sections 4.3.1/2/3/4/5/6/7 the effect of injection of alkyl alkoxy sulfates at a concentration of 100 ppm has been tabulated and discussed. The total experimental time of observation was eight hours. The results for the seven surfactants have been discussed in decreasing order of hydrophobicity.

4.3.1 ALFOTERRA G16-20S M (Hydrophobicity Rank: 1, PO(*m*) = 20, EO(*n*)= 0)

The system was injected with 100 ppm of the surfactant and left for over 16 hours in this case and the drop shape did not change. The drop between the tiles did not move. For this particular case, the system was tested with a concentration level of 1000ppm as well but it yielded the same result as at 100ppm. Hence the surfactant is deemed ineffective for our system of Yates crude oil and Limestone with synthetic Yates brine.

4.3.2 ALFOTERRA S23-13S 90 (Hydrophobicity Rank: 2, PO(*m*) = 13, EO(*n*)= 0)

Figure 14 is a photographic depiction of the effect of injection of 100ppm of ALFOTERRA 23S-13S 90 on the Yates crude oil drop with time at particular instances of the experiment. The dynamic contact angles are listed in Table 5 and Figure 15 depicts the change in the advancing angle with time.

It can be seen from Figure 14 that there is significant movement with respect to the big Yates oil drop on the surface of the lower crystal in the first 34.40 min after surfactant injection. The drop completely escapes from the lower crystal leaving behind a very small amount of the oil on its surface. The contact angle fluctuated around 155 degrees, hence there was no change in the wettability of the system yet and continued to remain strongly oil-wet.

The system was further allowed to interact and our focus was directed to the analysis of the formation of smaller droplets from the remaining oil on the lower crystal. We can see that the first such small drop begins to form at 63.10 min. This indicates that the surfactant molecules are finally in enough number that have lodged on to the interface between the limestone crystal surface and the oil droplet and/or between the oil droplet and brine. It finally escapes onto the upper crystal at 86 minutes. Only a part of the drop escapes from the lower crystal due to the adhesion force that exists between the Yates oil drop and the limestone crystal. The water advancing angle at this point fluctuated at around 154 signifying no alteration in the wettability of the system yet.

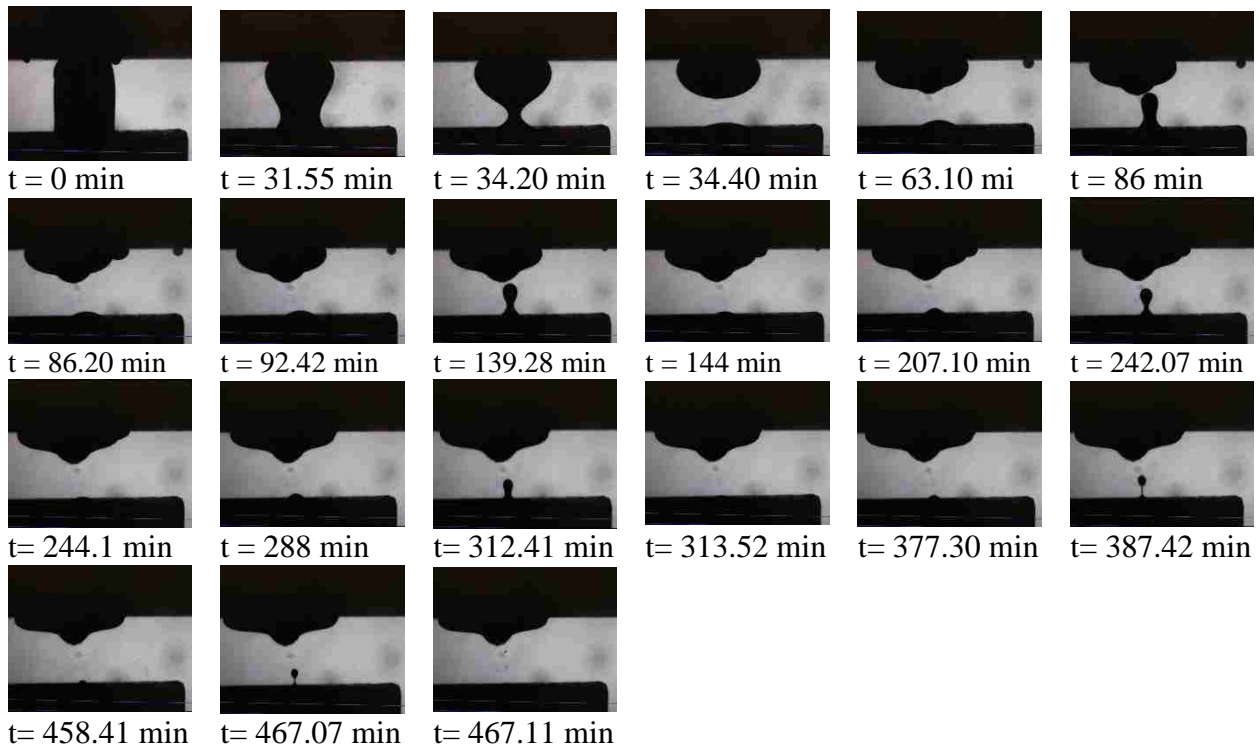


Figure 14: Photographic depiction of Yates oil drop dynamic behavior during injection of 100 ppm of ALFOTERRA S23-13S 90 surfactant.

A second droplet formation began forming at around 94.42 min and escaped at 139.28 min. This behavior of the Yates oil drop repeated itself at 242.07 min, 312.41 min, 387.42 min and at 467.07 min. At each of these instances the dynamic water advancing angles fluctuated around 153 degrees. Towards the end, the advancing angle slightly dropped to 148 degrees at 545 min and 685

min which was the instance for the last droplet to escape (Figures not shown). Hence, even though there was a slight change in the contact angle, the wettability of the system continues to remain strongly oil wet by the injection of 100 ppm of ALFOTERRA S23-13S 90.

Table 5: Dynamic Water Advancing Contact Angle for various times during injection of 100 ppm of ALFOTERRA S23-13S 90.

Time (min)	Θ_a (deg)
0	154
31.55	154
34.3	
63.1	155
86.2	
92.4	155
144	
207.7	150
244.1	
288.06	150
313.52	
377.3	153
458.41	153
545	148
685	148

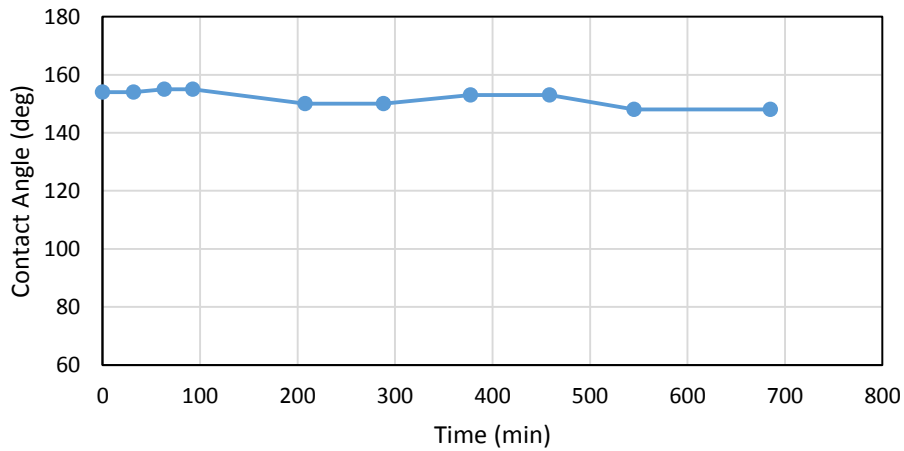


Figure 15: Variation of advancing dynamic contact angle with time during injection of 100 ppm of ALFOTERRA S23-13S 90M

4.3.3 ALFOTERRA S23-11S 90 (Hydrophobicity Rank: 3, PO(m) = 11, EO(n)= 0)

Figure 17 is photographic depiction of the effect of injection of 100ppm of ALFOTERRA S23-11S 90 on the Yates crude oil drop with time at particular instances of the experiment. The dynamic contact angles are listed in Table 6 and Figure 16 depicts the change in the advancing angle with time.

As can be seen that the drop between the two crystals escapes from the lower crystal within the first 1.15 min. This is much faster in comparison to Alf 13S which took approximately 34 min. A subsequent droplet formation can be seen at 7.40 min that escapes at 9.04 min. this cycle is repeated several times over at 19.56 min, 26.34 min, 31.46 min, 34.58 min, 41.24 min, 46.41 min, 51 min and finally at 113.15 min. It should be noted that the measured contact angles during the first 99 min was around 151 degrees. However eventually, the contact angles measured were close to a 100 degrees. This shows that the wettability has been altered and the system has changed from being a strongly oil wet system to intermediate wet. After the last droplet escaped at 113.15 min, another smaller drop was formed was at 124.4 min but did not leave the lower crystal thereby leaving some oil on the lower crystal.

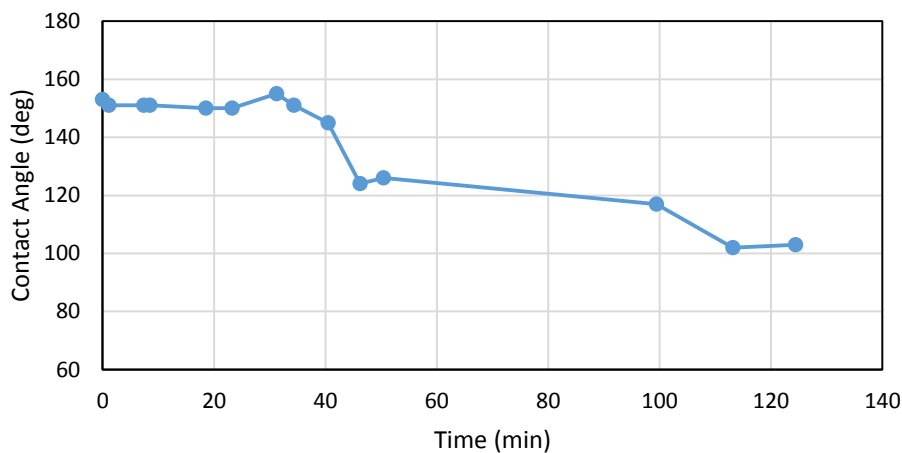


Figure 16: Variation of advancing dynamic contact angle with time during injection of 100 ppm of ALFOTERRA S23-11S 90.

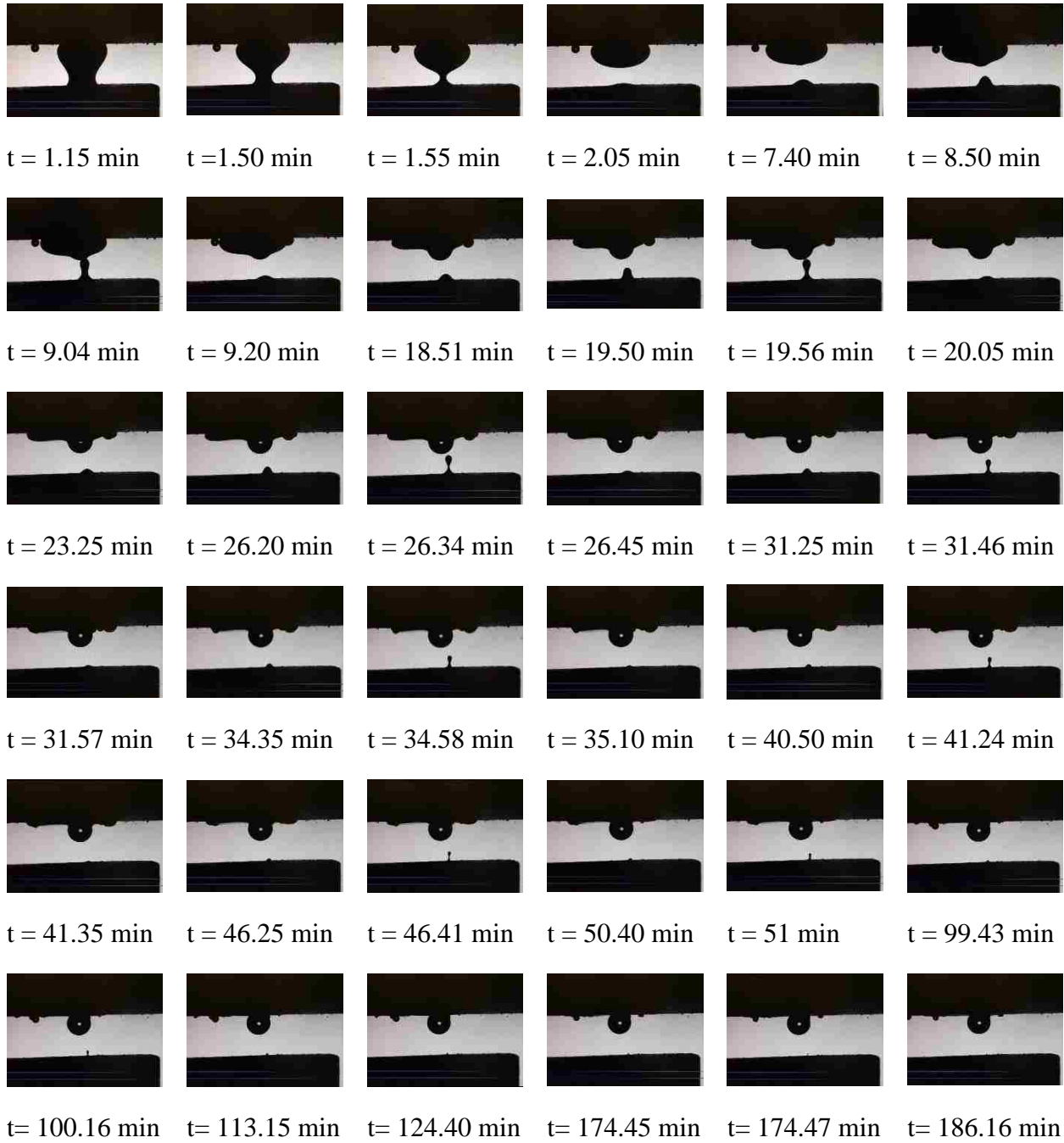


Figure 17: Photographic depiction of Yates oil drop dynamic behavior during injection of 100 ppm of ALFOTERRA S23-11S 90 surfactant.

Table 6: Dynamic Water Advancing Contact Angle for various times during injection of 100 ppm of ALFOTERRA S23-11S 90 surfactant.

Time (sec)	Θ_a (deg)
0	151
1.15	151
2.05	
7.40	151
8.50	153
9.20	
18.51	150
20.05	
23.25	150
26.45	
31.25	155
31.57	
34.35	151
35.10	
40.50	153
41.35	
46.25	124
50.40	126
99.43	117
113.15	102
124.4	103

4.3.4 ALFOTERRA S23-9S 90 (Hydrophobicity Rank: 4, PO(m) = 9, EO(n)= 0)

Figure 18 is a photographic depiction of the injection of 100 ppm of ALFOTERRA 23S-9S 90. Figure 19 and Table 7 lists the dynamic water advancing and receding angles at each instance of time. From Figure 18, we can see that the drop between the crystals escapes from the lower crystal on to the top crystal at the instance of 7.18 min. This is faster than both Alf 13S and 11S. After this point the cyclical formation of smaller drops begin to form and escape at various instances of time.



Figure 18: Variation of advancing dynamic contact angle with time during injection of 100 ppm of ALFOTERRA S23-9S 90M.

As can be seen, the water advancing angle reduces from an initial 152 to 135-140 in the first 22 min. However it is essential to note that subsequent droplets of the oil from the lower crystal did escape to upper tile of the system when left over an extended duration of time.

Table 7: Dynamic Water Advancing Contact Angle for various times during injection of 100 ppm of ALFOTERRA S23-9S 90.

Time (sec)	Θ_a (deg)
0	152
5	152
7	152
7.24	
12.4	153
13.1	
14.3	153
14.45	154
15	
16.15	150
16.43	153
17	
18.1	135
18.3	135
18.55	
20.11	135
20.45	
21.31	140
21.55	
22.3	142
22.45	
45.15	110
59.45	110
82.41	90
108.46	110
150	90
163	90
201	90
222	117
269.3	90
405	130

The subsequent smaller droplets had an advancing angle close to 90° as seen at the time instances 45.15 min, 59.45 min till 405 min. The last drop is formed at the instance of 405 min but

does not float away. Therefore some oil was definitely remaining on the lower tile but with the advancing angle reduced to almost 90 we can say that the wettability of the system was altered from extremely oil-wet to intermediate wet.

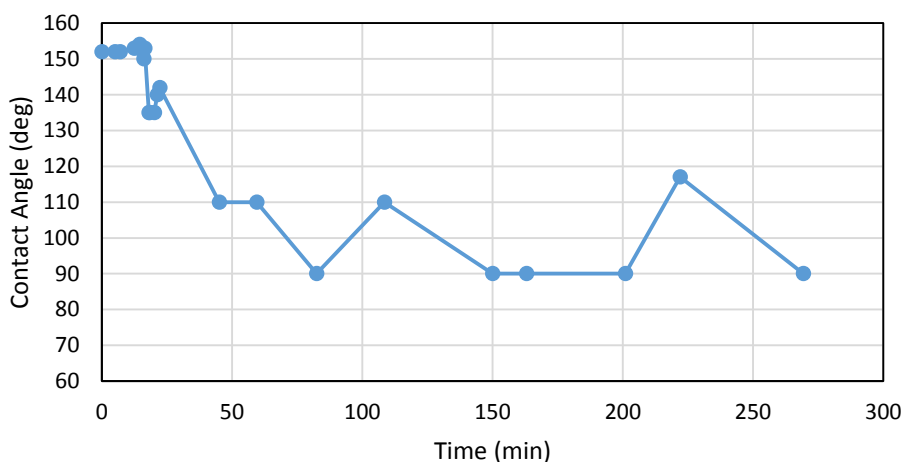


Figure 19: Variation of advancing dynamic contact angle with time during injection of 100 ppm of ALFOTERRA S23-9S 90M.

4.3.5 ALFOTERRA S23-7S 90 (Hydrophobicity Rank: 5, PO(*m*) = 7, EO(*n*)= 0)

Figure 20 is a photographic depiction of the injection of 100 ppm of ALFOTERRA 23S-7S 90. Table 8 and Figure 21 list the dynamic water advancing angles at each instance of time. As can be seen from Figure 20, the drop takes 26.30 min to escape from the lower crystal on to the upper crystal. This is considerably more time taken than both the 11S and 9S but less than the 13 S. This is probably an indication that the surfactant structures are slowly moving out of the ideal range of hydrophobicity for our particular system.

The water advancing angle reduces from about 170 degrees to 160 degrees during this time span. Beyond this duration we see the occurrence of the small droplet formation from the remaining oil on the lower crystal at the time instances of 32.48 min, 38.33 min, 44.23 min and 49.09 min. After 49.20 min, no changes of the remaining oil were seen to take place till the end of

the experiment at 451.36 min. The water advancing dynamic contact angle shifted close to 135 degrees which signifies that our system went from being strongly oil wet to weakly oil wet.

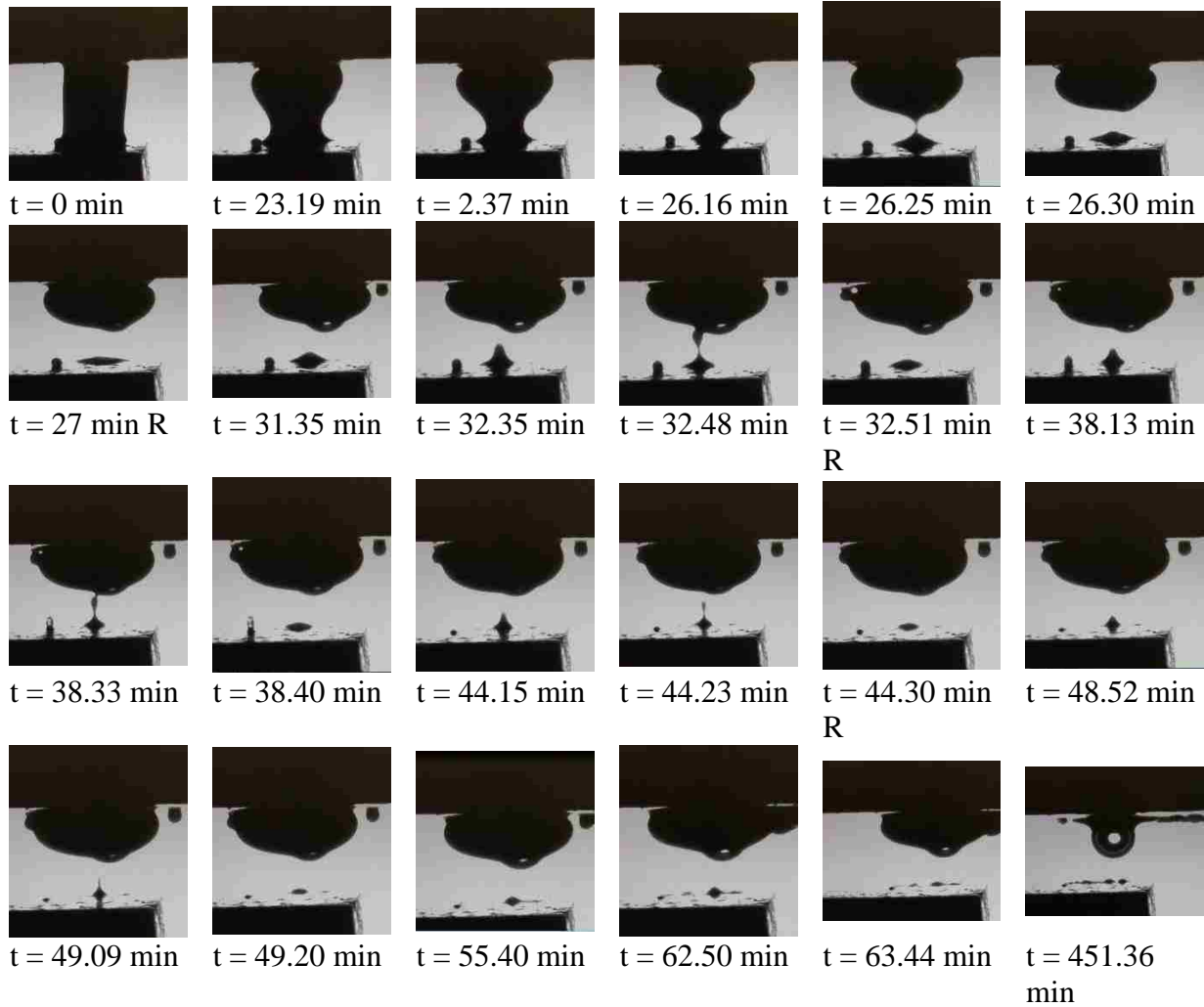


Figure 20: Dynamic Water Advancing Contact Angle for various times during injection of 100 ppm of ALFOTERRA S23-7S 90 surfactant.

Table 8: Dynamic Water Advancing Contact Angle for various times during injection of 100 ppm of ALFOTERRA S23-7S 90 surfactant.

Time (min)	Θ_a (deg)
23.19	170
24.37	170
26.16	160
27	
31.35	155
32.51	158
38.13	150
38.4	
44.15	144
48.52	135
49.2	
62.5	135

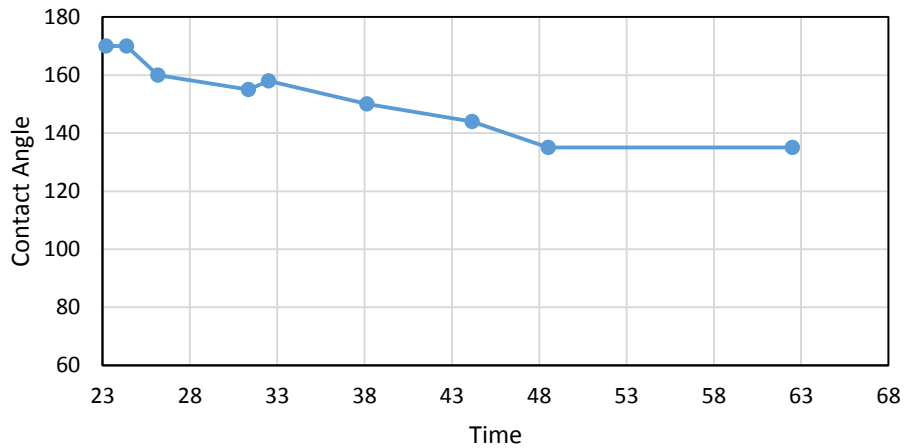


Figure 21: Variation of advancing dynamic contact angle with time during injection of 100 ppm of ALFOTERRA S23-7S 90M

4.3.6 ALFOTERRA K3-41S (Hydrophobicity Rank: 6, PO(m) = 4, EO(n)= 1)



t = 0 min



t = 470 min

Figure 22: Photographic depiction of Yates oil drop dynamic behavior during injection of 100 ppm of ALFOTERRA K3-41S surfactant.

Figure 22 shows the effect of the surfactant injection of 100 ppm of ALFOTERRA K3-41S. The system was left for 8 hours in this case and the drop shape did not change. The drop between the crystals did not move. This is an indication that the surfactant is now definitely out of the favorable hydrophobicity range. We can infer this since the structure of this surfactant is similar in all aspects to the ones discussed in the previous sections. The only change being the number of PO and EO units it carries which directly affects the hydrophobic nature of the surfactant.

4.3.7 ALFOTERRA K45-DS (Hydrophobicity Rank: 7, PO(m) = 0, EO(n)= 3)

Figure 23 shows the effect of the surfactant injection of 100ppm of ALFOTERRA K45-DS. The system was left for approximately 7hr 33 min in this case and the drop shape did not change. The system remained static. It should be noted here that this in accordance with the study by Rao et al., 2006 wherein the anionic surfactant tested was an ethoxy sulfate with 3 EO units and it resulted in a reversed wettability. That is the system became even more oil wet.

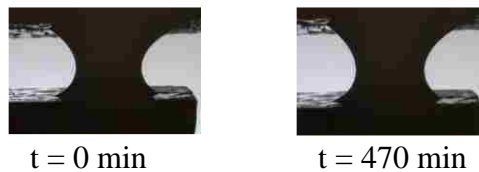


Figure 23: Photographic depiction of Yates oil drop dynamic behavior during injection of 100 ppm of ALFOTERRA K45-DS surfactant.

4.4 Interfacial tension measurements of ALFOTERRA

In section 4.3, it is apparent that only ALFOTERRA 7S, 9S, 11S and 13S had any effect on our system even though they were structurally similar to the rest of the surfactants tested in the ALFOTERRA family. It can be deduced that these four surfactants fall within the favorable range of hydrophobicity with respect to our particular system. We also note that surfactants 9S and 11S were effective in altering the wettability of the system. We see a repeat phenomenon of the small droplet (SD) formation over an extended period of time with the dynamic contact angles being close to 90 degrees for the droplets formed towards the end of each of the experiments. To confirm this phenomenon as being an effect of wettability alteration and not because of a further reduction of the IFT, we conducted IFT measurements as a fraction of time for the above mentioned four surfactants, ALFOTERRA 7S, 9S, 11S and 13S. All measurements were made via the spinning drop technique at the Sasol laboratory testing facility at Lake Charles.

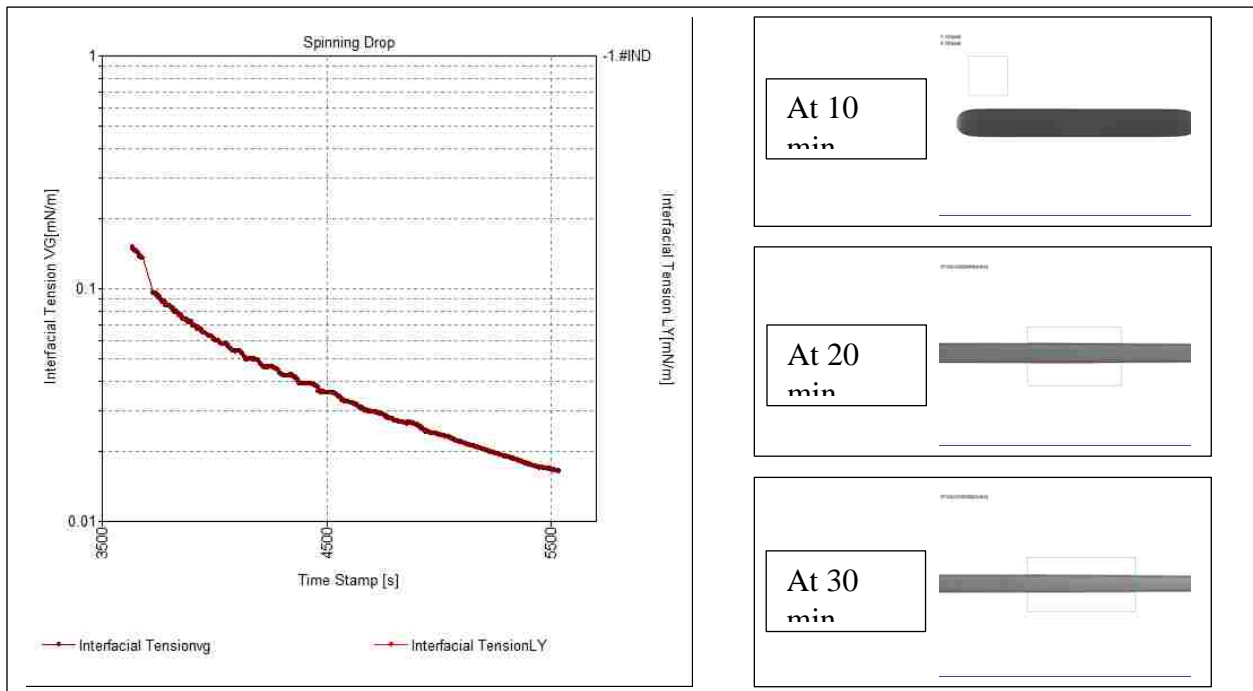


Figure 24: Graphical presentation of IFT variation with time for ALFOTERRA 13S with pictorial depiction of the behavior of the crude oil sample at various instances during testing.

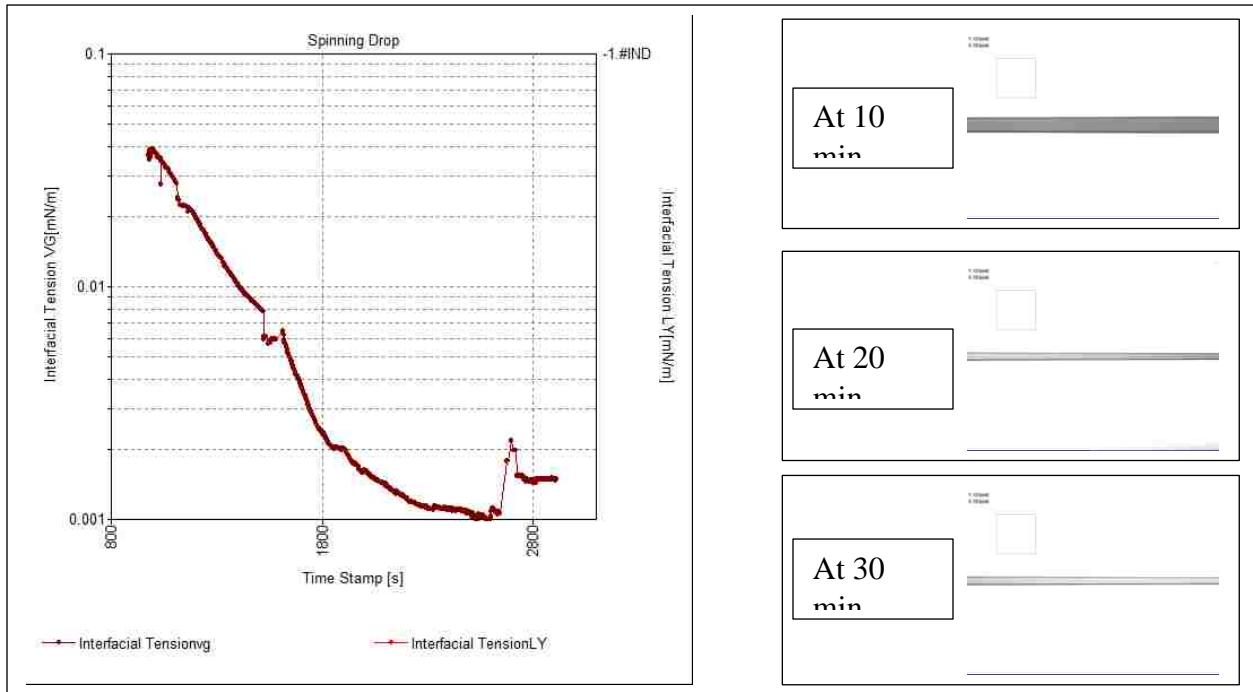


Figure 25: Graphical presentation of IFT variation with time for ALFOTERRA 11S with pictorial depiction of the behavior of the crude oil sample at various instances during testing.

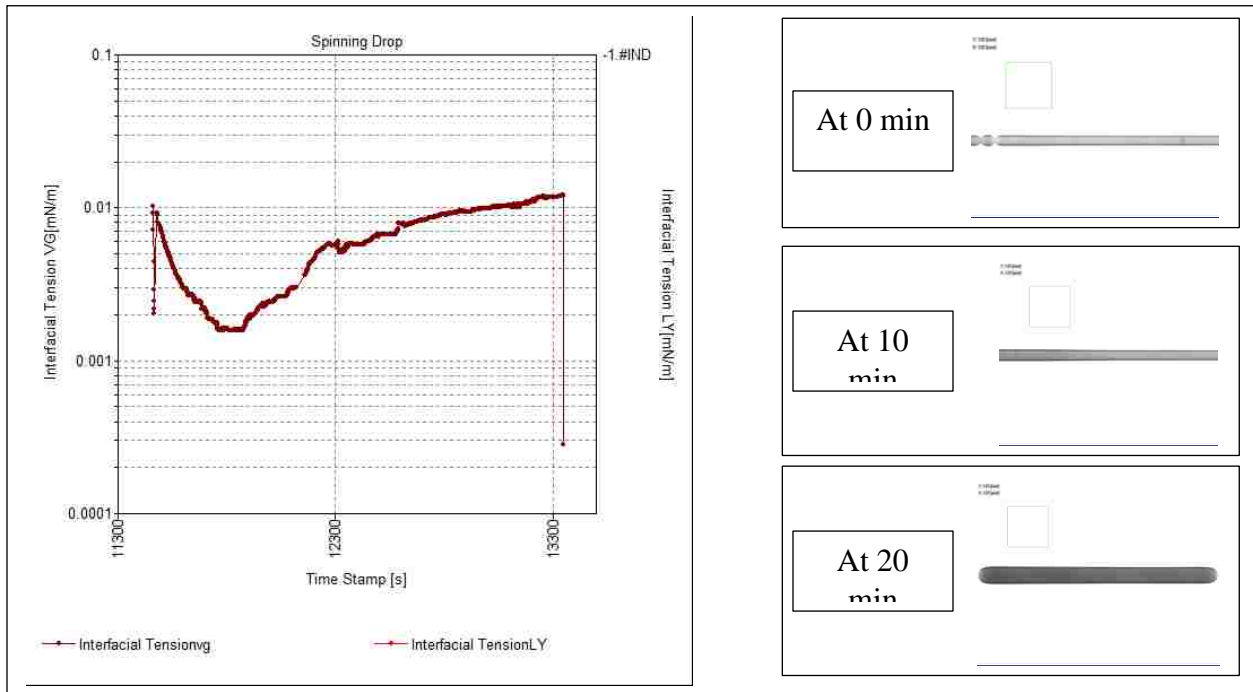


Figure 26: Graphical presentation of IFT variation with time for ALFOTERRA 9S with pictorial depiction of the behavior of the crude oil sample at various instances during testing.

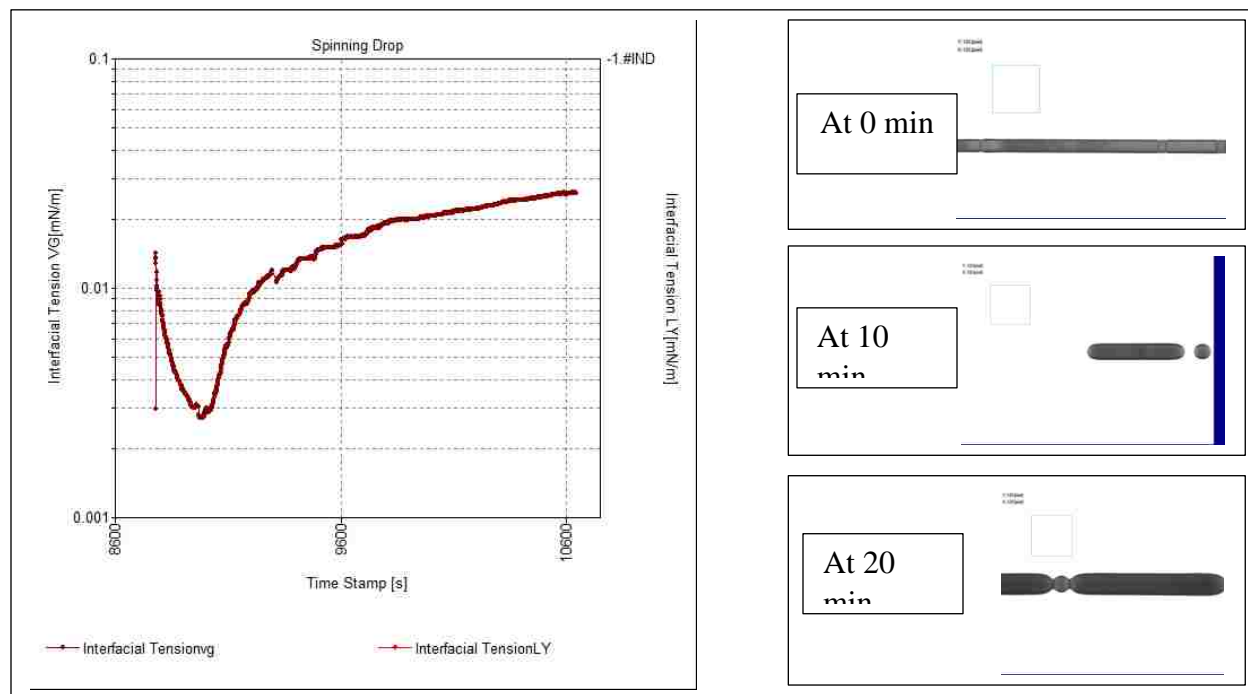


Figure 27: Graphical presentation of IFT variation with time for ALFOTERRA 7S with pictorial depiction of the behavior of the crude oil sample at various instances during testing.

- From the respective graphs and the actual tabulated data, we see that the IFT for ALFOTERRA 13S kept decreasing with time and stabilized eventually at 0.0165 mN/m in about 30 min. It should be noted that there was an almost linear decrease in the IFT with time, the difference between the initial 0.15 mN/m and final 0.015mN/m was about an order of magnitude with the average IFT being 0.0476 mN/m.
- The IFT reduction for ALFOTERRA 11S was substantially lower than 13S. The IFT stabilized at 0.0015 mN/m and the average IFT was 0.0069 mN/m.
- In the case of ALFOTERRA 9S, the IFT first dropped to values of 0.0015 mN/m but then started increasing linearly with the final recorded value at 0.012 mN/m. The average value was 0.0063 mN/m.

- A trend similar to 9S was seen in ALFOTERRA 7S. The IFT first fell to around 0.0028 mN/m and then peaked towards the end at 0.026 mN/m. The average IFT was 0.016mN/m

There is definitely a trend in the IFT reduction from the above data. We can infer that ALFOTERRA 11S and 9S structurally provide the right level of hydrophobicity while 13S is too hydrophobic and 7S is too hydrophilic. The significance of this on our system and its wettability will be discussed in section 4.7

4.5 Effect of injection of Alkyl Ether Carboxylates (SOLOTERRA) at a concentration of 100ppm

In the subsequent sections, namely sections 4.5.1/2/3/4/5, the effect of injection of alkyl ether carboxylates at a concentration of 2000 ppm have been tabulated and discussed. The total experimental time of observation was again eight hours. The results for the five surfactants have been discussed in decreasing order of hydrophobicity.

4.5.1 SOLOTERRA 960 (Hydrophobicity Rank: 1, PO(*m*) = 4.5, EO(*n*)= 2)

Figure 28 is the photographic depiction of the effect of the surfactant SOLOTERA 960 when injected into our system at a concentration level of 2000 ppm. As seen, it took approximately 54 min for the oil drop between the crystals to escape to the top crystal. Unfortunately any dynamic contact angle measurement for this particular surfactant was not possible due to the cloudy nature of the surfactant that affected the transparency level. However, it was visually noticeable that no further small oil droplets escaped from the remaining oil on the lower crystal until towards the end of the experiment at 434.47 min.

Even though no contact angle measurements were done for this particular run, it can be comprehended that the surfactant was not all too effective for our system just by taking into the

account the time it took for the oil droplet to leave the lower crystal and also the fact that no smaller droplets were formed during the period of our experiment except for one instance.

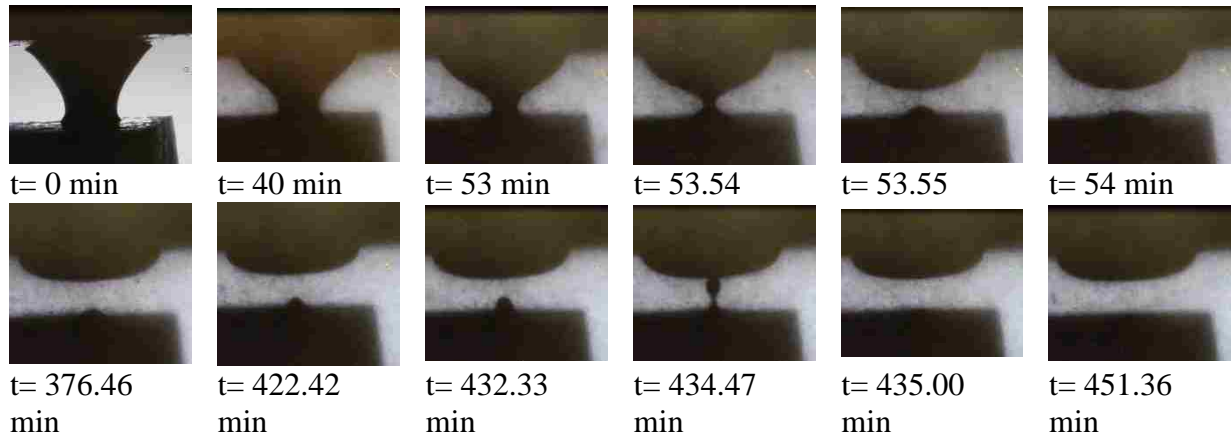


Figure 28: Photographic depiction of Yates oil drop dynamic behavior during injection of 2000 ppm of SOLOTERRA 960 surfactant.

4.5.2 SOLOTERRA 961 (Hydrophobicity Rank: 2, $PO(m) = 4.5$, $EO(n) = 5$)

Figure 29 is the photographic depiction of the effect of the surfactant SOLOTERRA 961 when injected into the system at same concentration level of 2000 ppm. It can be seen that the oil droplet escapes from the lower crystal in less than the first 3 minutes. We see a subsequent small droplet formation beginning at about 50 minutes and finally escapes at 179 minutes and no further change in the system was seen. However the contact angle measure at each of these instances is approximately around 165 degrees. The wettability of the system did not change.

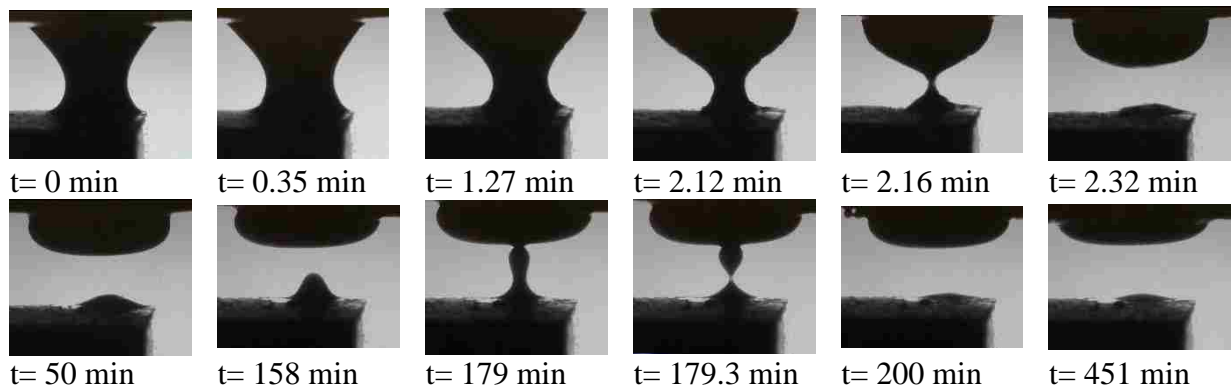


Figure 29: Photographic depiction of Yates oil drop dynamic behavior during injection of 2000 ppm of SOLOTERRA 961 surfactant.

Table 9: Dynamic Water Advancing Contact Angle for various times during injection of 2000 ppm of SOLOTERRA 961 surfactant.

Time (min)	Θ_a (deg)
0.35	165
1.27	165
2.32	167
158	165
179	165

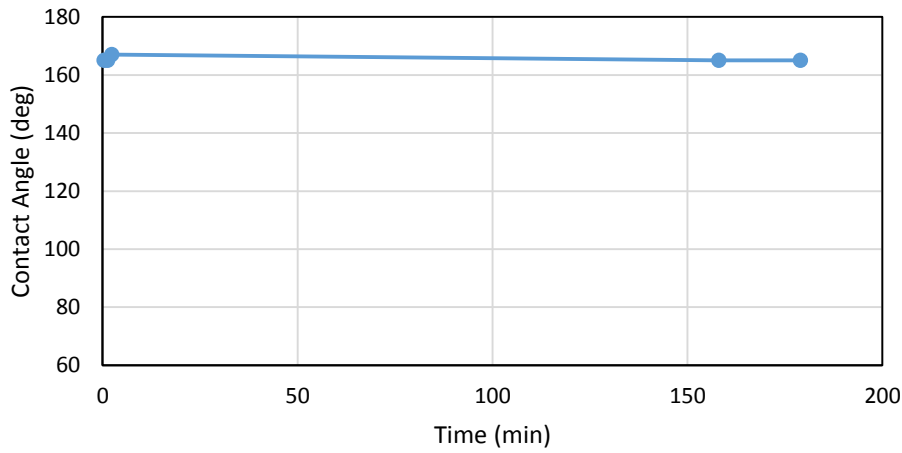


Figure 30: Variation of advancing dynamic contact angle with time during injection of 2000 ppm of SOLOTERRA 961.

4.5.3 SOLOTERRA 939 (Hydrophobicity Rank: 3, $PO(m) = 1.6$, $EO(n) = 2.4$)

Figure 31 is the photographic description of the injection of 2000 ppm of SOLOTERRA 939 and Table 10 lists the dynamic advancing contact angle for the period of approximately 7 and half hours. Figure 32 is the graphical representation of the change in dynamic water advancing contact angle with time.

As can be seen, the drop between the two crystals escapes to the top crystal within the first 18 minutes leaving behind a reasonable amount of oil on the lower crystal. Subsequently it can be seen that the residual oil droplet rises at 24.06 min but then falls back again at 26 min. The droplet attempts to escape again by beginning to rise at 27.50 min but falls back again. In this case the

phenomenon of small droplet formation is not seen even over extended periods of time at 2000ppm as has been seen previously several times in the ALFORTERRA group of surfactants at a concentration level of 100ppm.

Hence the remaining oil drop on the lower crystal remains stagnant till the end as can be seen in the photographic description with no change in contact angle. Hence the surfactant was ineffective in altering the wettability of the system and continues to remain extremely oil wet.

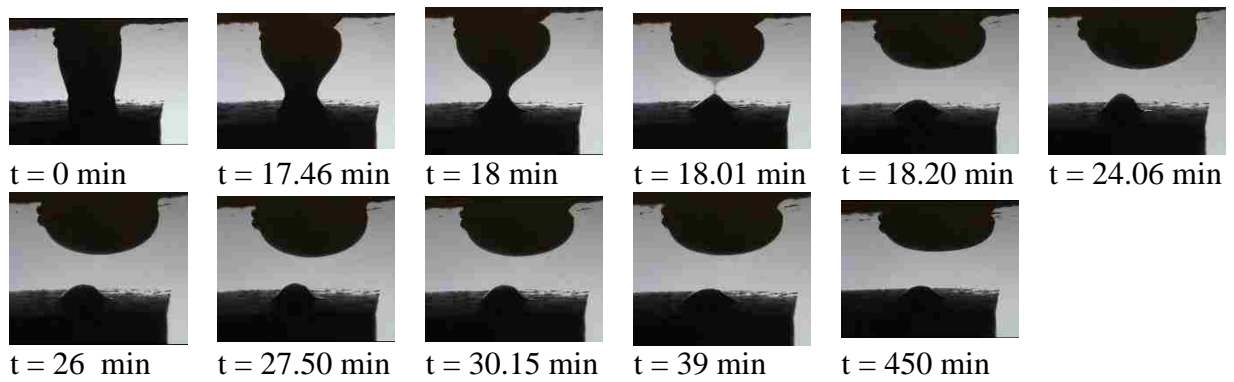


Figure 31: Photographic depiction of Yates oil drop dynamic behavior during injection of 2000 ppm of SOLOTERRA 939 surfactant.

Table 10: Dynamic Water Advancing Contact Angle for various times during injection of 2000 ppm of SOLOTERRA 939.

Time (min)	Θ_a (deg)
17.46	148
18	148
18.2	143
24.06 rise	149
26 fall	147
27.5 rise	154
30.15 fall	140
39	141

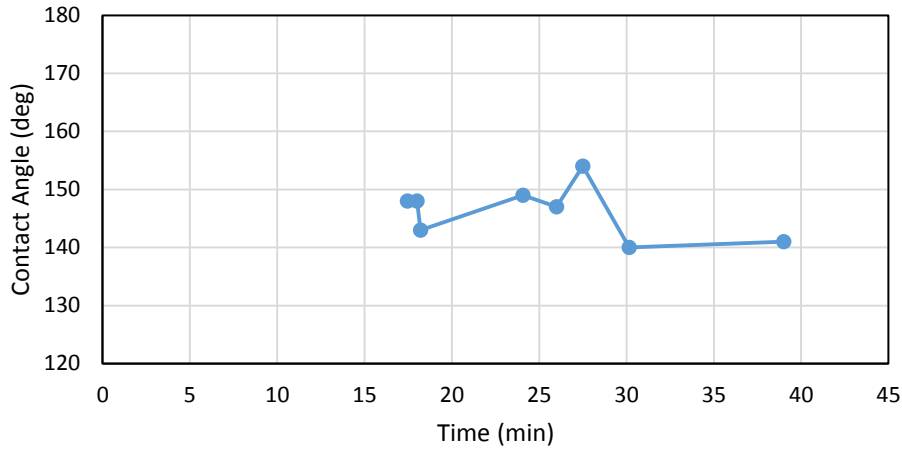


Figure 32: Variation of advancing dynamic contact angle with time during injection of 2000 ppm of SOLOTERRA 939.

4.5.4 SOLOTERRA 970 (Hydrophobicity Rank: 4, PO(m) = 3, EO(n)= 7)

Figure 33 is the photographic description of the injection of 2000 ppm of SOLOTERRA 970 and Table 11 lists the dynamic advancing contact angle for the period of our experimental time which was 7 and half hours. Figure 34 is the graphical representation of the water advancing contact angle variation with time.

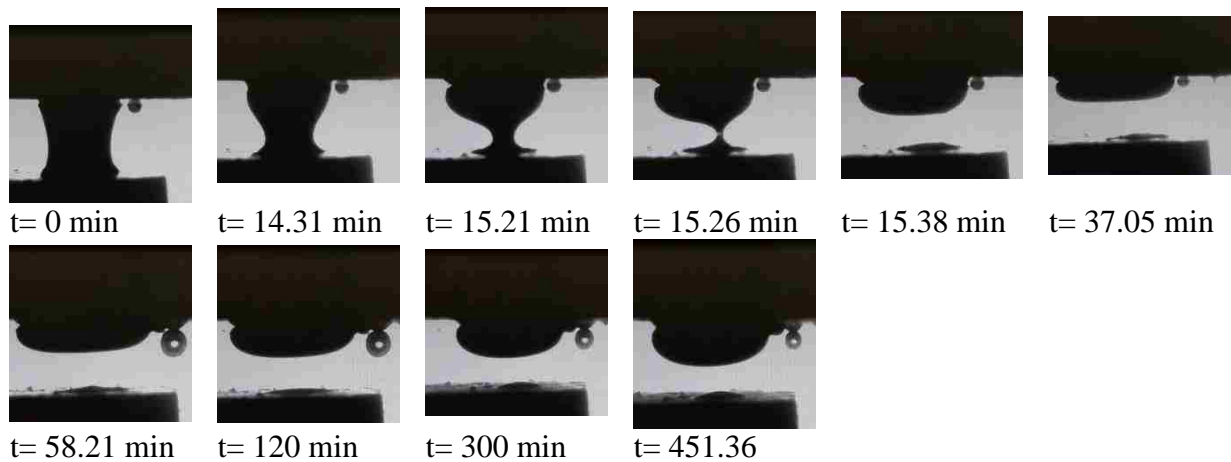


Figure 33: Photographic depiction of Yates oil drop dynamic behavior during injection of 100 ppm of SOLOTERRA 970 surfactant.

With the injection of the surfactant, the oil drop left the lower crystal and floated away to the upper crystal within the first 16 minutes. However post that, as can be seen in the photographic depiction, there was no change or movement in the system. We fail to see any small droplet formation over the entire length of the experimental time, signifying that there was no wettability alteration encountered by the system.

Table 11: Dynamic Water Advancing Contact Angle for various times during injection of 2000 ppm of SOLOTERRA 970.

Time (min)	Θ_a (deg)
14.31	155
15.21	165
15.38	
120	162
300	160

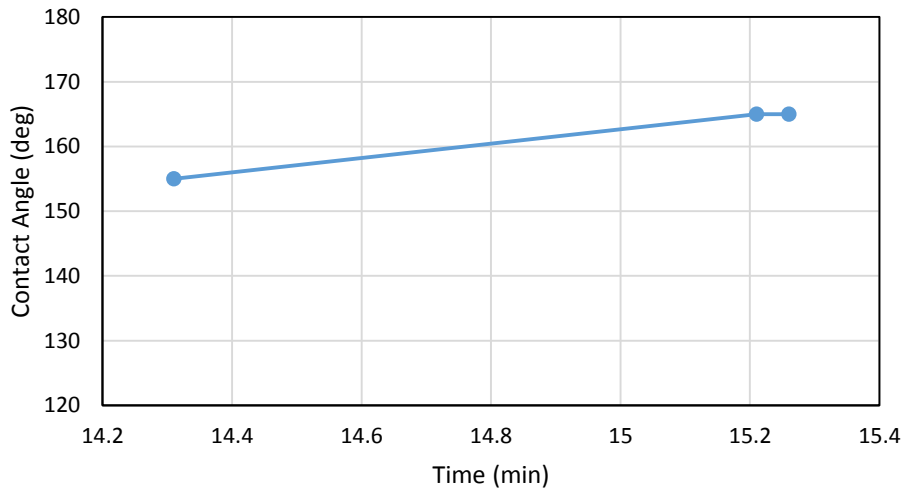


Figure 34: Variation of advancing dynamic contact angle with time during injection of 2000 ppm of SOLOTERRA 970.

4.5.5 SOLOTERRA 938 (Hydrophobicity Rank: 5, $PO(m) = 0$, $EO(n) = 7$)

Figure 35 is the photographic description of the injection of 2000 ppm of SOLOTERRA 939 and Table 12 list the dynamic advancing contact angle for the period of approximately 7 and

half hours. Figure 36 is the graphical representation of the water advancing contact angle variation with time.

The drop between the two crystals escaped from the lower crystal in the first 9 minutes, which is much faster than SOLOTERRA 939. At 23.17 min, a smaller droplet escaped from the remainder oil on the lower crystal. Subsequent smaller droplet formations were seen at 23.54 min, 24.14 min, 24.43 min and 25.16 min. the system remained stagnant after 25.16 min until the end which is 450 min. The dynamic water advancing contact angle hovered around 160 degrees and did not change until the end of the experiment.

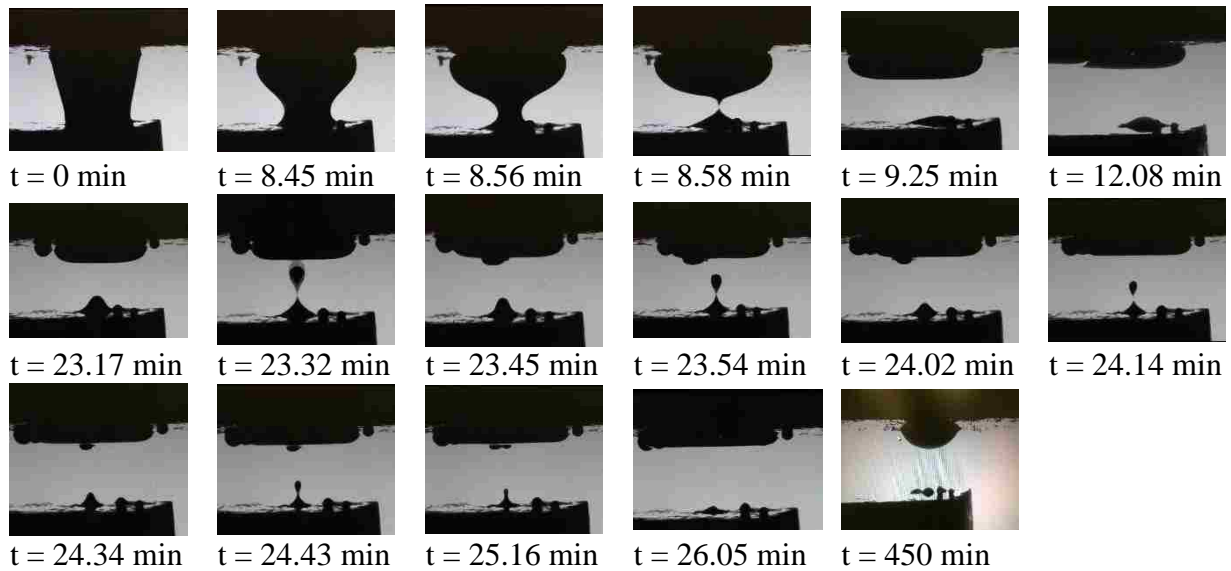


Figure 35: Photographic depiction of Yates oil drop dynamic behavior during injection of 2000 ppm of SOLOTERRA 938 surfactant.

Table 12: Dynamic Water Advancing Contact Angle for various times during injection of 2000 ppm of SOLOTERRA 938.

Time (min)	Θ_a (deg)
8.45	158
8.56	158
12.08	160
23.17	159
23.45	168
24.02	167
24.34	156
25.16	161

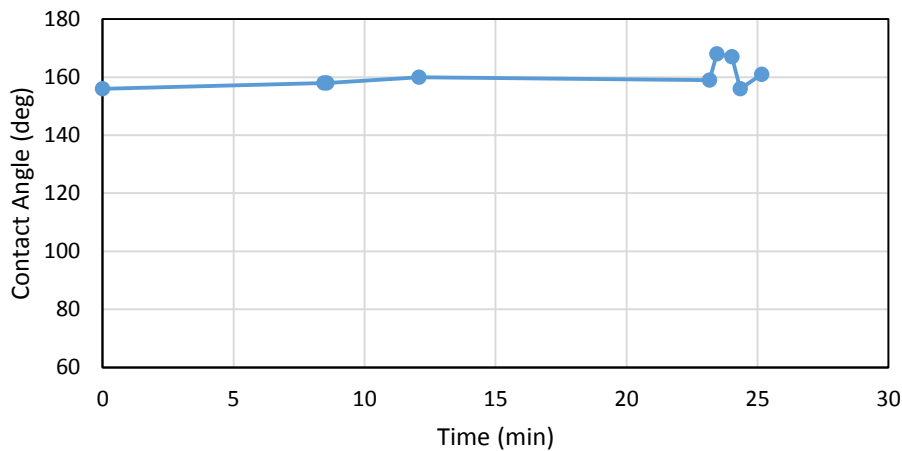


Figure 36: Variation of advancing dynamic contact angle with time during injection of 2000ppmof SOLOTERRA 938.

4.6 Interfacial Tension Measurements for SOLOTERRA

IFT measurements were also made for the five surfactants listed in section 4.5, all belonging to the SOLOTERRA family. None of the surfactants were effective in wettability alteration in terms of contact angles measured nor did the surfactants exhibit any small droplet formation, except for SOLOTERRA 938. The IFT measurements were done in an effort to investigate this nature of the surfactant keeping in mind the possibility that these surfactants might not be as effective as the ALFOTERRA in terms of IFT reduction as well.

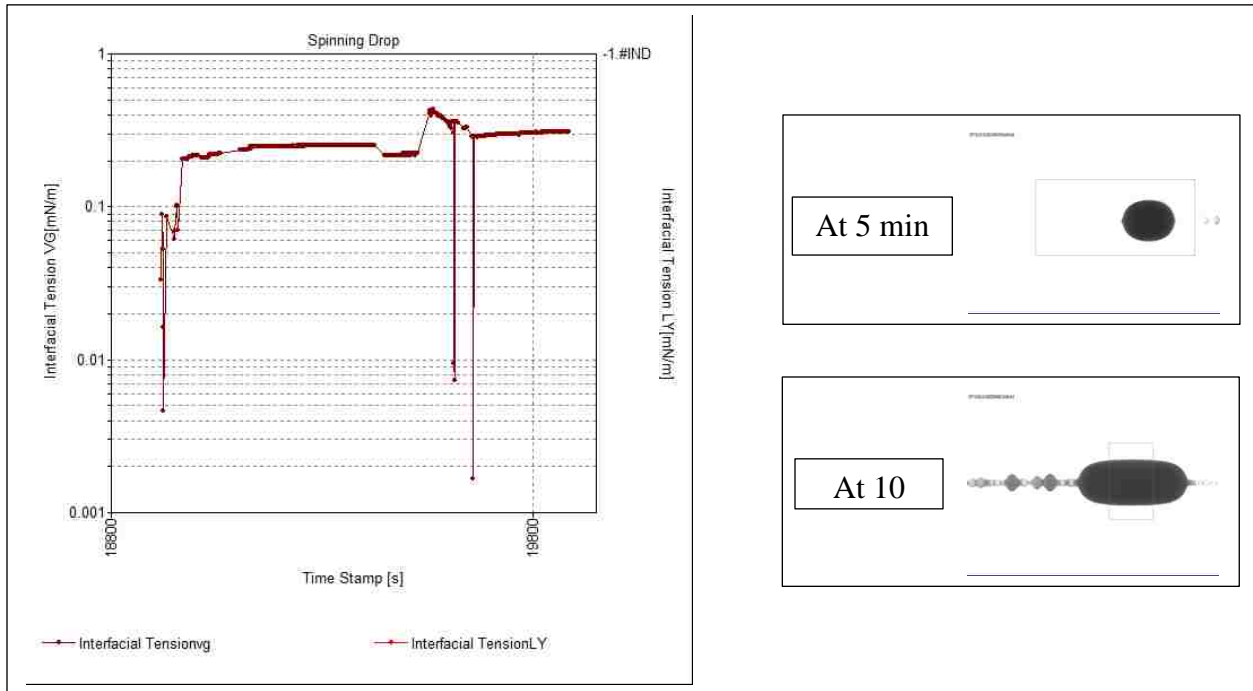


Figure 37: Graphical presentation of IFT variation with time for SOLOTERRA 960 with pictorial depiction of the behavior of the crude oil sample at various instances during testing.

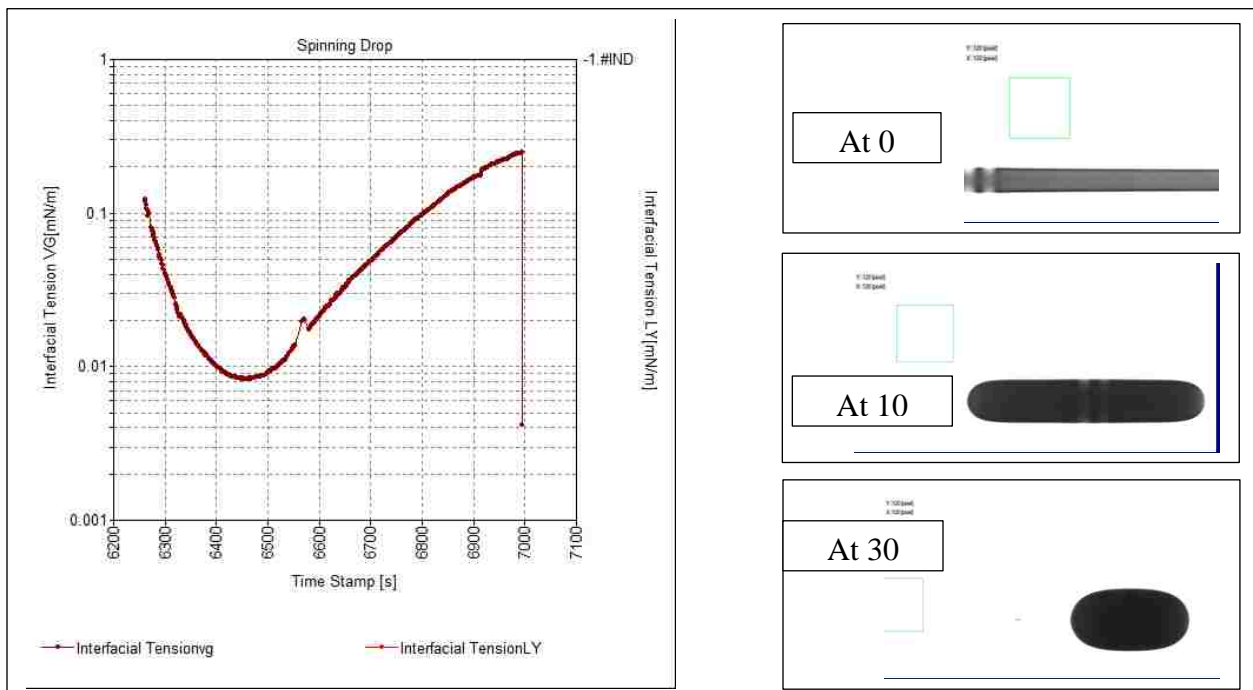


Figure 38: Graphical presentation of IFT variation with time for SOLOTERRA 961 with pictorial depiction of the behavior of the crude oil sample at various instances during testing.

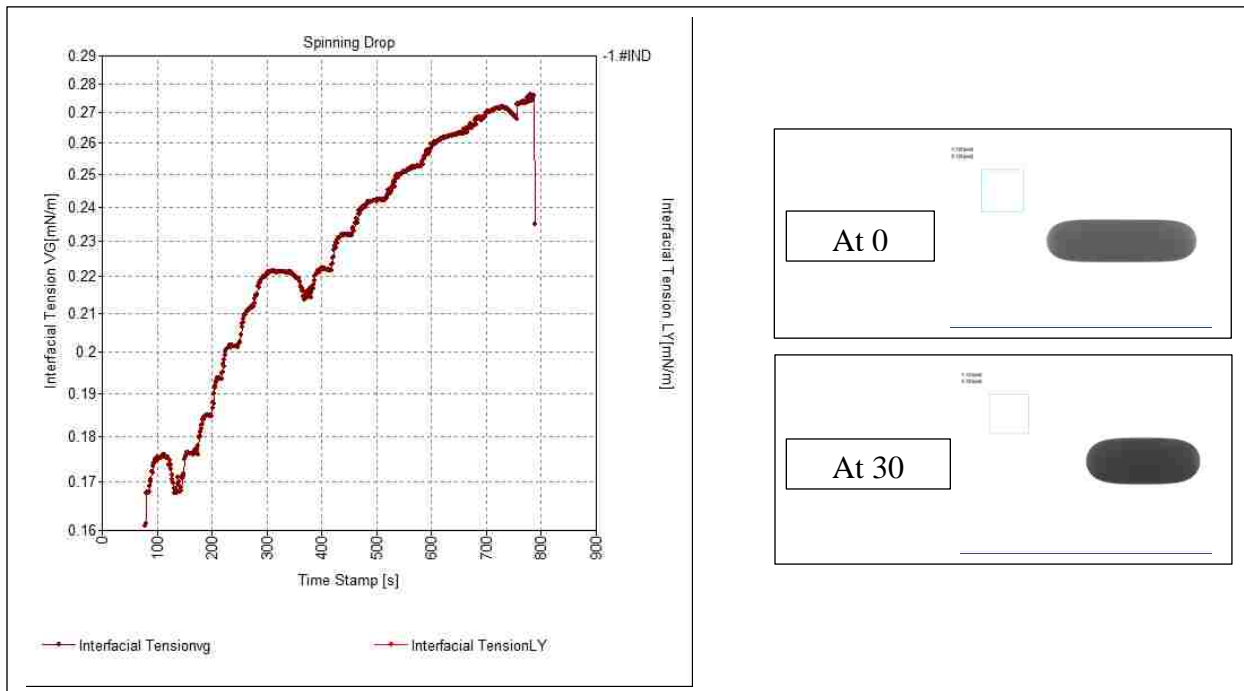


Figure 39: Graphical presentation of IFT variation with time for SOLOTERRA 970 with pictorial depiction of the behavior of the crude oil sample at various instances during testing.

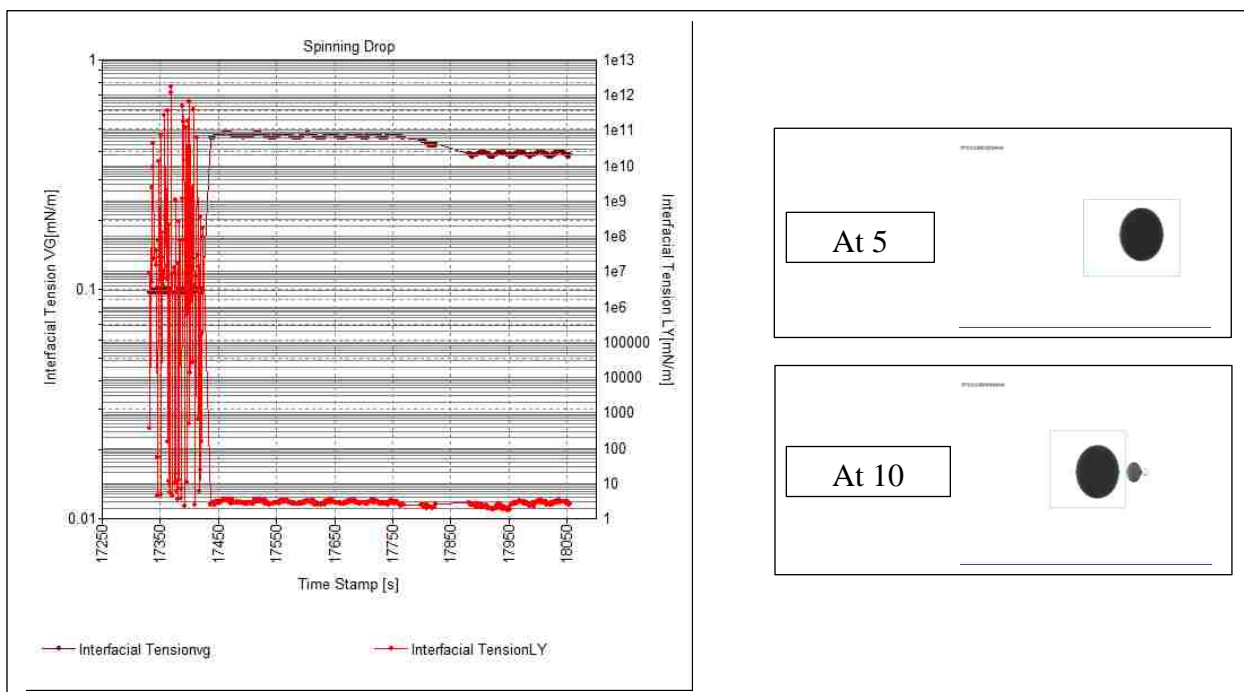


Figure 40: Graphical presentation of IFT variation with time for SOLOTERRA 938 with pictorial depiction of the behavior of the crude oil sample at various instances during testing.

- For SOLOTERRA 960, we see that in Figure 37 the interfacial tension does not reduce as much in comparison to the ALFOTERRAs in general. The IFT remained close to 0.30 mN/m.
- In the case of SOLOTERRA 961, the IFT value first fell with the lowest measured value at 0.0082 mN/m however it then started rising back and stabilized at values of about 0.246 mN/m.
- SOLOTERRA 970 showed an upward trend right from the beginning with the last recorded value for our test being 0.27 mN/m
- The IFT values for SOLOTERRA 938 were mostly consistent around 0.38 mN/m.
- The recorded IFT values for SOLOTERRA 939 fluctuated around 0.30 mN/m.

All the above measurements were done via the spinning drop technique at the Sasol laboratory testing facility in Lake Charles.

4.7 Bond number (N_B) analysis during surfactant injection

Bond number, defined as the ratio of gravity forces to capillary forces (Ayirala et al., 2006), has been calculated for the surfactant samples in this section. Since our study involved the measurement of both water advancing contact angle (θ_a) as well as interfacial tension (σ), the dimensionless Bond number (N_B) helps define the rock-fluids interactions induced by changes in advancing contact angle (or wettability) and oil-water interfacial tension in our system quantitatively. It was calculated for the four surfactants (ALFOTERRA 13S, 11S, 9S and 7S) which showed small droplet formation. The Bond number calculated in this section is defined as (Ayirala et al., 2006),

$$N_B = \frac{\delta\rho g(h - h_i)d}{\sigma \cos\theta} \quad (5)$$

Where N_B is the Bond number, σ is the interfacial tension in mN/m, $\delta\rho$ is the density difference in gm/cc, g is the acceleration due to gravity (cm/s^2), D is the drop diameter in cm and θ is the water advancing contact angle in degrees. The initial height of the oil drop between the crystals is represented by h_i while h is the height of the neck formed, measured from the lower crystal.

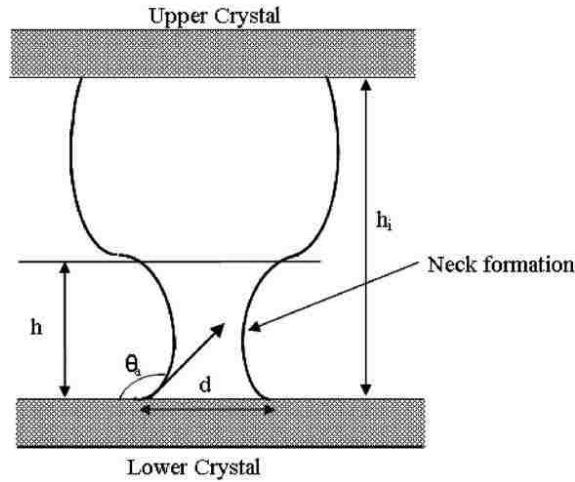


Figure 41: Schematic presentation of the equilibrium drop between the two crystal surfaces (Ayirala et al., 2006)

$$\tau = \sigma \cos\theta \quad (6)$$

Equation 6 is the equation for the work of adhesion, where τ is the work of adhesion, σ is the oil-water interfacial tension and θ is the contact angle. The work of adhesion defines the adhesive force between the oil drop and the crystal. When compared to equation 5 for Bond number, we can replace the denominator with τ . This helps us compare the buoyancy force (numerator), that enables the drop to leave the lower crystal surface, to the adhesive force (denominator) that prevents the drop from floating away from the crystal surface. As a result, the drop is unstable on the crystal surface for as long as the Bond number is above unity which implies the buoyancy force is greater than the adhesive force. Once the Bond number falls below unity the drop becomes stable as now the adhesive force between the drop and the crystal is greater than the buoyancy force. Hence the calculation of Bond number is of great significance since it takes into

account all the forces acting on the oil drop and helps explain the oil drop movement better quantitatively. Since both contact angle and IFT are changing due to surfactants used and N_B combines both these variables, Bond number is a better indicator of the overall effect of the surfactants used and thus serves well to compare different surfactants tested in this study.

Table 13: Quantitative drop dynamics and calculated bond numbers for the oil drop on the lower crystal during the injection of 100 ppm of Alfoterra 13S.

T (min)	Θ_a (rad)	Θ_a (deg)	d (cm)	h (cm)	N_B ($\times 10^2$)	Drop dynamics on lower crystal
31.55	2.687805	154	0.553	0.248	22.05	Neck formation
34.2	2.879791	165	0.553	0.248	20.52	Neck about to shear
34.4	2.879791	165	0.553	0.074	28.68	Drop sheared
86.2	2.722711	156	0.322	0.0137	18.64	Residual drop rising
139.28	2.705258	155	0.24	0.0132	17.50	Residual drop rising
242.07	2.617992	150	0.172	0.0952	9.60	Residual drop rising
312.41	2.617992	150	0.129	0.074	8.59	Residual drop rising
387.42	2.705258	155	0.087	0.053	4.97	Residual drop rising
467.07	2.705258	155	0.055	0.05	3.16	Smaller drop rising

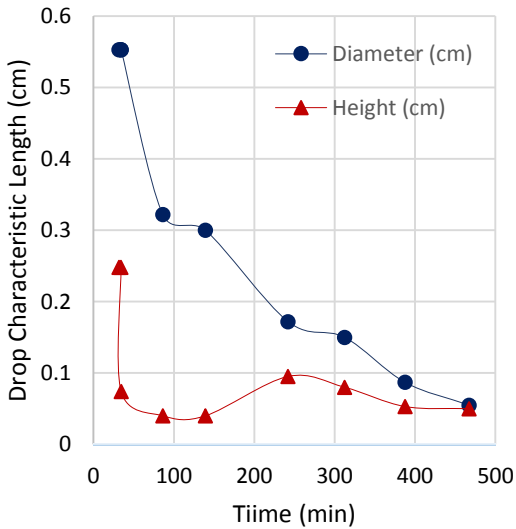


Figure 42: Variation of drop dimensions with time for the drop on the lower crystal during the injection of 100 ppm of Alfoterra 13S.

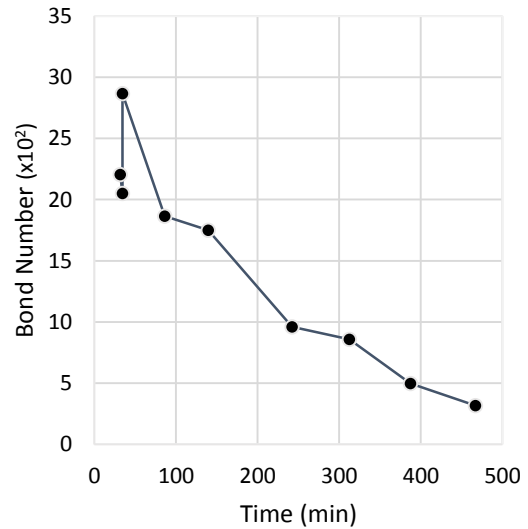


Figure 43: Variation of bond numbers with time for the drop on the lower crystal during the injection of 100 ppm of Alfoterra 13S.

Table 14: Quantitative drop dynamics and calculated bond numbers for the oil drop on the lower crystal during the injection of 100 ppm of Alfoterra 11S.

T (min)	Θ_a (rad)	Θ_a (deg)	d (cm)	h (cm)	N_B ($\times 10^2$)	Drop dynamics on lower crystal
1.15	2.635445	151	0.457	0.182	187.50	Neck formation
1.55	2.705258	155	0.315	0.182	124.72	Neck about to shear
2.05	2.879791	165	0.407	0.047	202.48	Drop sheared
9.04	2.705258	155	0.233	0.105	110.10	Residual drop rising
19.56	2.705258	155	0.2012	0.1031	95.45	Residual drop rising
26.34	2.617992	150	0.167	0.0899	85.21	Residual drop rising
31.46	2.617992	150	0.115	0.0714	60.89	Residual drop rising
34.58	2.635445	151	0.092	0.0608	49.24	Residual drop rising
46.25	2.164206	124	0.097	0.0608	81.20	Residual drop rising
100.16	2.042034	117	0.0318	0.0345	34.45	Smaller drop rising
186	1.832594	105	0.013	0.021	25.31	Drop stable

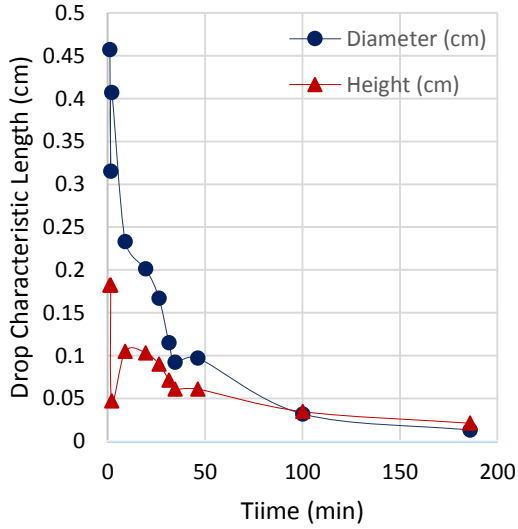


Figure 44: Variation of drop dimensions with time for the drop on the lower crystal during the injection of 100 ppm of Alfoterra 11S.

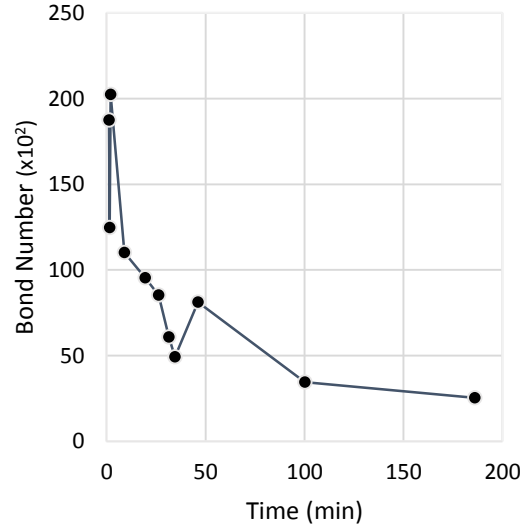


Figure 45: Variation of bond numbers with time for the drop on the lower crystal during the injection of 100 ppm of Alfoterra 11S.

Table 15: Quantitative drop dynamics and calculated bond numbers for the oil drop on the lower crystal during the injection of 100 ppm of Alforterra 9S.

T (min)	Θ_a (rad)	Θ_a (deg)	d (cm)	h (cm)	N_B ($\times 10^2$)	Drop dynamics on lower crystal
5.0	2.652898	152	0.611	0.206	25.27	Neck formation
7.0	2.652898	152	0.35	0.156	16.71	Neck about to shear
14.45	2.687805	154	0.222	0.0899	12.25	Residual drop rising
16.43	2.670352	153	0.145	0.063	8.57	Residual drop rising
20.33	2.356193	135	0.1	0.058	7.52	Residual drop rising
22.4	2.478365	142	0.093	0.037	6.56	Residual drop rising
45.5	1.919861	110	0.0318	0.018	5.37	Smaller drop rising
82.41	1.570795	100	0.023	0.016	7.67	Smaller drop rising
163	1.570795	100	0.058	0.026	18.97	Smaller drop rising
223.16	2.042034	117	0.058	0.023	7.30	Smaller drop rising
269.58	1.570795	100	0.045	0.021	14.87	Smaller drop rising
405	2.268926	130	0.042	0.02	3.76	Drop stable

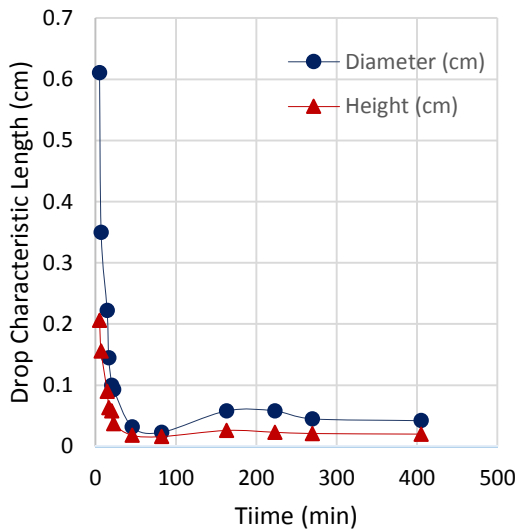


Figure 46: Variation of drop dimensions with time for the drop on the lower crystal during the injection of 100 ppm of Alforterra 9S.

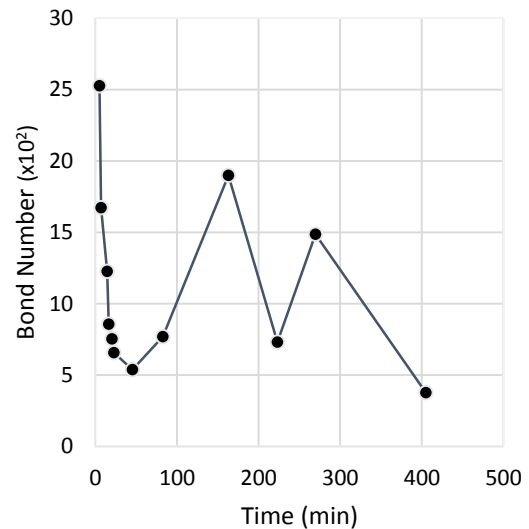


Figure 47: Variation of bond numbers with time for the drop on the lower crystal during the injection of 100 ppm of Alforterra 9S.

Table 16: Quantitative drop dynamics and calculated bond numbers for the oil drop on the lower crystal during the injection of 100 ppm of Alforterra 7S.

T (min)	Θ_a (deg)	d (cm)	h (cm)	N_B ($\times 10^2$)	Drop dynamics on lower crystal
23.19	170	0.69	0.3095	14.23	Neck formation
24.37	170	0.597	0.291	12.90	Neck narrowing
26.16	160	0.462	0.275	10.87	Neck narrowing
26.26	165	0.457	0.148	13.58	Neck about to shear
27	165	0.5	0.148	14.86	Drop sheared
32.48	158	0.2963	0.1719	8.78	Residual drop rising
38.33	150	0.19	0.1296	6.51	Residual drop rising
44.23	144	0.156	0.1269	5.75	Residual drop rising
49.09	140	0.116	0.0899	4.81	Residual drop rising
62.5	135	0.158	0.0688	7.34	Appears to be rising
451.36	135	0.14	0.058	6.61	Appears to be rising

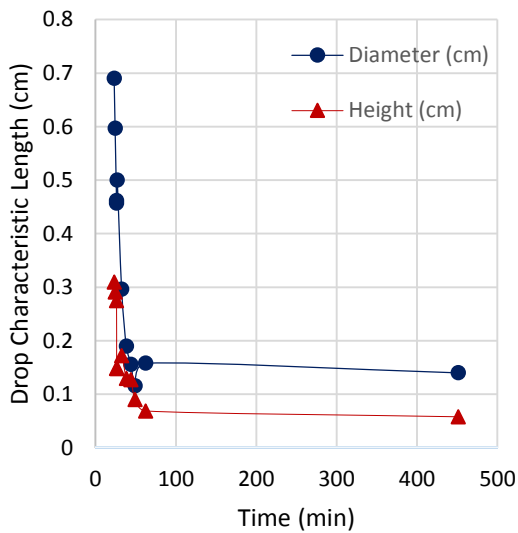


Figure 48: Variation of drop dimensions with time for the drop on the lower crystal during the injection of 100 ppm of Alforterra 7S.

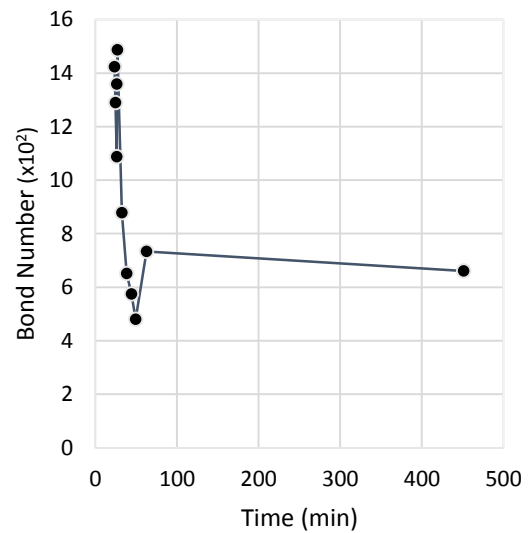


Figure 49: Variation of bond numbers with time for the drop on the lower crystal during the injection of 100 ppm of Alforterra 7S.

During the injection of Alfoterra 13S it is seen in Table 13 that the Bond number stays above unity (meaning that the buoyancy force was larger than interfacial force) until the end of the experimental duration, implying that there is a possibility of residual drops rising from the lower crystal beyond the recorded 467 minutes. It has been seen that the IFT recorded for 13S was 0.016 mN/m and this surfactant did not show much effect on the wettability of the system, with water advancing contact angles measuring close to 150 degrees. Hence even though the Bond number is well above unity at 467 minutes and shows that the drop is unstable on the lower crystal, 13S can be concluded to definitely have an effect on our rock fluids system in terms of droplet movement, but not an efficient surfactant sample in terms of the IFT reduction as well as wettability alteration. The surfactant is also slow in having an effect on the system when compared to the other 3 surfactants as can be seen in the Bond number comparative plot in Figure 50. It took 31.5 minutes for the oil drop to show neck formation.

For Alfoterra 11S, the Bond numbers are really high. This is because of the really low IFT recorded (0.0015 mN/m) during the injection of 100 ppm of Alfoterra 11S. As a result the drop has a high Bond number of 2,500 even at 186 min, at which point in our experiment, little or no residual oil was seen to exist on the lower crystal. This indicates that the surfactant is highly efficient and well suited to our system of Yates oil - Yates synthetic brine – Limestone. The system is unstable even though most of the oil has left the lower crystal. This implies that system is in a state where oil would be easily recoverable. This can be attributed to both the altered wettability, as seen through the measured water advancing contact angle of 103 degrees, as well as the reduced interfacial tension of 0.0015 mN/m. The effectiveness of the surfactant can also be seen in Figure 50. It took comparatively less time for the oil drop between the crystals to form a neck (1.15 min).

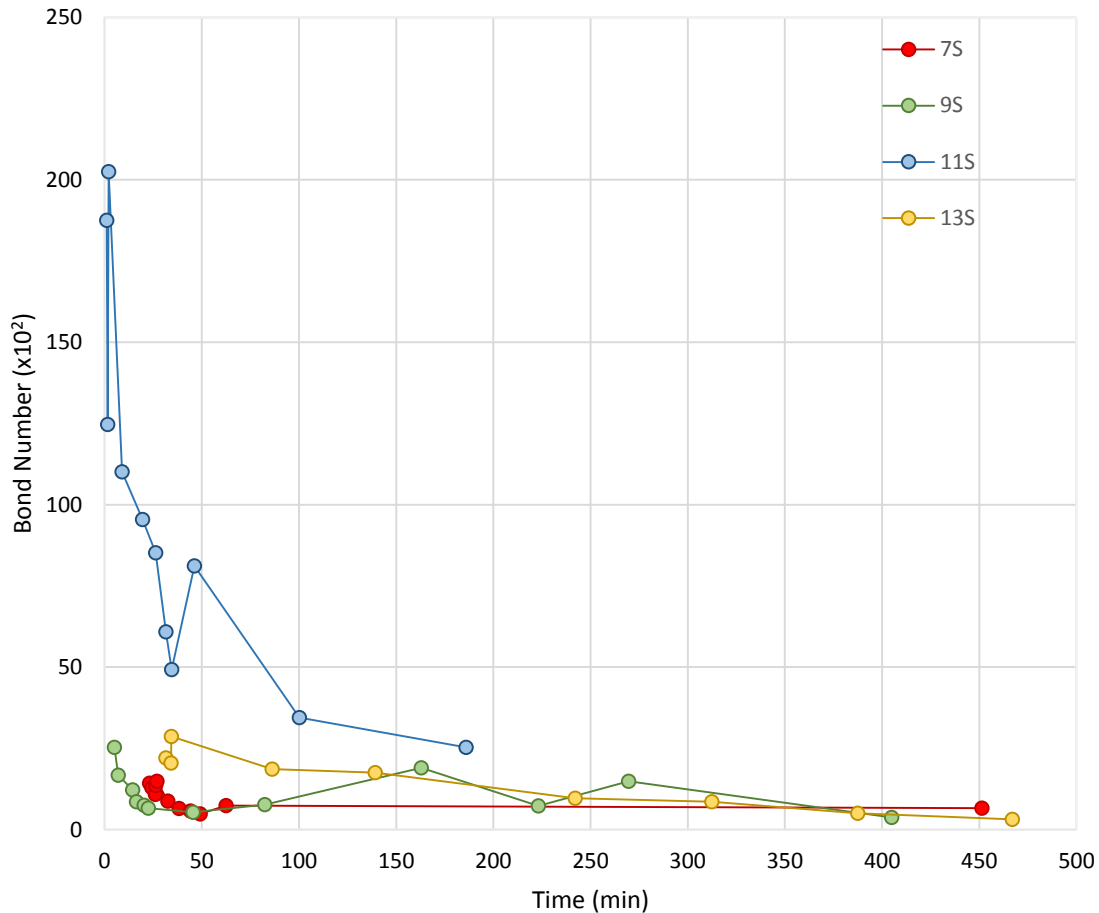


Figure 50: Bond number comparative plot for Alfoterra 13S, 11S, 9S and 7S as a factor of time.

Alfoterra 9S had a similar effect on the system as is evident from the Bond numbers listed in Table 15. It did not show as high a variation as in the case of Alf 11S since the IFT reduction was less (0.012 mN/m) and differed by one order of magnitude. The drop was unstable at the end of 405 minutes and had a Bond number of 376. Hence this surfactant is definitely suited for our system but when compared to Alf 11S, it is not as efficient. Alf 11S recorded a Bond number as high as 2,500 at just 186 min while Alf 9S has a Bond number of 300 after 405 minutes. Since both the surfactants altered the wettability from a strongly oil-wet system to an intermedia-wet system with similar measured contact angles ($90^{\circ} - 100^{\circ}$), the difference in the Bond numbers can be safely attributed to the interfacial tension reductions by the respective surfactants. However it

would not be apt to conclude that Alf 11S is better suited than 9S because the concentrations of the surfactants used in this study was just 100 ppm. This is a much lower concentration than what is used in the field (2500-5000 ppm), at which point the IFT reductions by both surfactants may or may not be that different. It should also be noted that at the time instances of 82.41 min, 163 min and 269.58 min the oil droplets escaping from the lower crystal were too small for the contact angles to be measured. Visually it could be deduced that the angles were close to 90 degrees. However in Table 15, we have used $\theta_a = 100^\circ$. This is because if $\theta_a = 90^\circ$ is used then $\cos\theta_a$ in eqn. (5) would give us a Bond number of infinity.

Finally, during the injection of 100 ppm of Alfoterra 7S it was previously seen from the measured water advancing contact angles that the wettability of the system changed mildly from strongly oil wet to weakly oil wet ($\theta_a = 135^\circ$). This is further evident from the Bond number variation seen in Table 16 the drop is unstable and will continue to rise and escape with time as can be seen clearly at the time instant 451.36 min in Figure 20. However the effect of the surfactant on our system is sluggish and time taking and hence it does not appear to be the best surfactant for our particular rock fluids system. The effect of Alf 7S is similar to that of 13S. This can be seen from Figure 50. The neck formation in the oil drop begins only after 23 min. Therefore 7S does not appear to be the best suited surfactant for our rock fluids system.

4.8 Summary of results and observations

A total of 12 surfactants were tested on the rock fluids system of Yates crude oil-Yates synthetic brine-limestone. All twelve surfactants belonged to the anionic family. Of the twelve surfactants, seven were alcohol ethoxy sulfates or the trade name, ALFOTERRA. The rest five were alkyl ether carboxylates or the trade name, SOLOTERRA. The ALFOTERRAs and the

SOLOTERRAs were tested in decreasing order of hydrophobicity using the DDDC contact angle technique for determining wettability alteration.

From the results obtained we see that Alf G16-20S M with the highest level of hydrophobicity and Alf K3-41S & K45-DS with the least level of hydrophobicity were completely ineffective. Not only did we not witness any wettability alteration but it did not have any effect on our system as a whole. The Yates crude oil drop remained stationary between the upper and lower crystals.

Table 17: List of tested surfactants

S.N.	Surfactant	PO units	EO units	Hydrophobicity Rank
1	ALFOTERRA G16-20S M	20	0	1 (strongest)
2	ALFOTERRA® S23-13S 90	13	0	2
3	ALFOTERRA® S23-11S 90	11	0	3
4	ALFOTERRA® S23-9S 90	9	0	4
5	ALFOTERRA® S23-7S 90	7	0	5
6	ALFOTERRA K3-41S	4	1	6
7	ALFOTERRA K45-DS	0	3	7 (weakest)
8	SOLOTERRA 960	4.5	2	1 (strongest)
9	SOLOTERRA 961	4.5	5	2
10	SOLOTERRA 939	1.6	2.4	3
11	SOLOTERRA 970	3	7	4
12	SOLOTERRA 938	0	7	5 (weakest)

The remaining four surfactants did affect our system. As seen in section 4.3, the time taken for the oil droplet to escape the lower crystal during injection of 100 ppm of Alf 13S was 34.4 minutes. This reduces drastically to 1.55 min during injection of 100 ppm of Alf 11S. It slightly increased again to 7.18 min during injection of Alf 9S. And with the injection of Alf 7S, the time went back up again to 26.30 minutes. A trend can definitely be observed here. The four ALFOTERRAs differ in their structure with respect to the number of propylene oxide with Alf 13S, 11S, 9S and 7S having 13, 11, 9 & 7 PO units respectively. Clearly Alf 13S is too

hydrophobic for the system while Alf 7S is too hydrophilic to be effective in altering the rock fluids interaction in terms of wettability for this system.

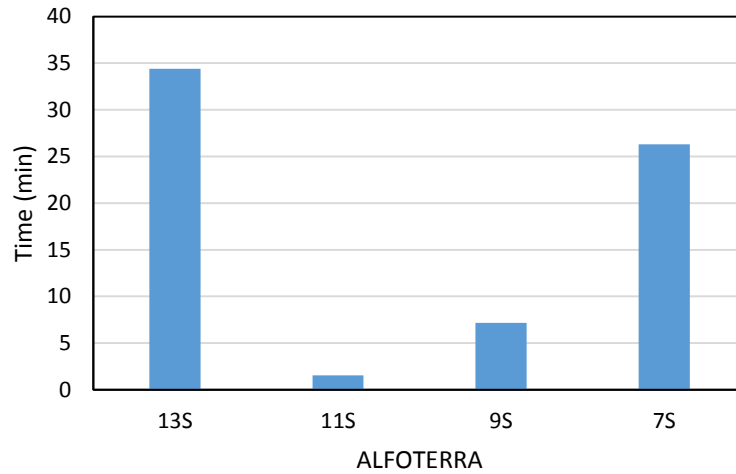


Figure 51: Duration of time for the initial Yates crude oil droplet to leave the lower crystal during injection of 100 ppm of the four ALFOTERRAs

In each of the four surfactants (13S, 11S, 9S, 7S) we see the phenomenon of small droplet formation after a certain period of time, in which the system and the surfactant had interacted. However, in the case of Alf 13S the small droplet formation was very limited to just six instances and was widely spread over the 450 minutes of our experimental time. The final dynamic contact angle measured was 150° , thereby showing no change in the wettability. The case was significantly different in Alf 11S and 9S. In both cases the small droplet formation was much more dominant. Oil droplets kept escaping from the residual oil on the lower crystal within short time intervals of each other. The final dynamic water advancing contact angle measured during the injection of 100 ppm of Alf 11S was 103° and for Alf 9S was approximately 90° . Hence, the wettability of our system was effectively changed from oil-wet to intermediate-wet. A similar effect was seen during the injection of Alf 7S. However the contact angle did not change as much. The small droplet formation was not as dominant either and the final dynamic contact angle measured was 135° signifying that the wettability had changed from oil-wet to weakly oil-wet.

In this study, the small droplet formation is of significance it can be correlated to the possibility of the surfactants interacting with the oil and brine phases as well as the rock surface resulting in a change in the wettability. During any surfactant flood, the recovery from a reservoir is dependent on a lot of factors related to the performance of the surfactant. The recovery depends on its adsorption by the reservoir rock, interfacial tension reduction in addition to wettability alteration. The effect of IFT reduction is one of the more pre-dominant characteristics of a surfactant and also more immediate. Therefore in our DDDC technique, the initial drop escaping the lower crystal can be attributed more due to the instant reduction of IFT as soon as the surfactant is introduced and less due to any possible wettability change. Wettability alteration is not as an instant phenomenon as IFT reduction. Therefore the subsequent small droplet formation can be attributed more due to the slowly altering wettability of the system than IFT reduction. To verify this, IFT measurements for these four surfactants were carried out as a function of time. From section 4.4 it is evident that the interfacial tension fell within the first few seconds of injection and remained stable over time. No drastic further reductions were seen, instead some actually exhibited slight increments. Therefore we can safely conclude that the subsequent small droplet formations and their departure seen during the course of these experiments were due to the slowly altering wettability. It should be further noted that the IFT reduction was about the same in all four cases of the ALFOTERRA surfactants varying slightly (0.016 mN/m, 0.001 mN/m, 0.012 mN/m and 0.026 mN/m for Alf 13S, 11S, 9S and 7S respectively). Yet the small droplet formation was seen more in Alf 11S and 9S and not in the cases of Alf 13S or 7S. This reinforces the fact that it is the wettability alteration capacity of the surfactant that matters more in the formation of smaller droplets seen over extended periods of experimental time and not the IFT reduction which manifests in the first few minutes.

An interesting fact to note is that the last surfactant tested in the ALFOTERRA group, K45-DS had three EO units and no PO units, making it much more hydrophilic than the rest. As discussed already it had no preferential wettability alteration to our system. Rao et al., (2006) tested a similar surfactant with 3 EO units in its structure. The anionic ethoxy sulfate surfactant used, resulted in reverse wettability alteration on the Yates reservoir system. The system became even more oil wet and showed gradual decrements in oil recoveries were due to the strongly oil-wet state induced by the surfactant.

We then tested surfactants from the SOLOTERRA group or the alkyl ether carboxylates. Each of these surfactants were a structural combination of both propylene oxide and ethylene oxide units. Even though the SOLOTERRAs are structurally completely different from the ALFOTERRA, they are in general more hydrophilic than all the ALFOTERRAs tested. Since Alf K3-41S and K45-DS were already well below the favorable range of hydrophobicity for our system, it was no surprise that the SOLOTERRAs in general were ineffective in altering wettability. The interfacial tension reduction was also not as much as the ALFOTERRA group and were higher by one order of magnitude. The values were 0.03 mN/m, 0.24 mN/m, 0.30 mN/m, 0.27 mN/m and 0.38 mN/m for Sol 960, 961, 939, 970 and 938 respectively. Small droplet formations were seen during the injection of three of the five SOLOTERRA surfactants but the process was much more sluggish with only a few time instances of droplet formation being encountered. No preferential wettability alteration in terms of contact angle measurements were seen in them.

In section 4.8 we saw the combined effect of both wettability alteration and interfacial tension reduction by calculating the Bond number at different time instances, for the surfactants which had an effect on our rock-fluids system namely Alfoterra 7S, 9S, 11S and 13S. Since both

contact angle and IFT are changing due to the surfactants used and N_B combines both these variables, Bond number helped quantify the overall effect of the surfactants used and was used as a comparative tool to compare the different surfactants tested in this study. During the injection of Alfoterra 13S it was seen that the Bond number stayed above unity until the end of the experimental duration. With a measured IFT of 0.016 mN/m and no wettability alteration, even though the Bond number stayed well above unity at 467, 13S can be concluded to be an effective surfactant for our system. With Alfoterra 11S, the Bond numbers calculated were really high due to the extremely reduced IFT and the altered wettability of the system to intermediate-wet. As a result the drop had a high Bond number of 2,500 even at 186 min, at which point in our experiment, little or no residual oil was seen to exist on the lower crystal. Therefore the surfactant is highly effective and well suited to our system of Yates oil - Yates synthetic brine – Limestone. Alfoterra 9S had a similar effect on the system as 11S. The drop was unstable at the end of 405 minutes and had a Bond number of 376. Hence this surfactant is definitely suited for our system as well. As for Alfoterra 7S, Table 16: Quantitative drop dynamics and calculated bond numbers for the oil drop on the lower crystal during the injection of 100 ppm of Alfoterra 7S.. The drop was unstable and would continue to rise and escape with time as was seen clearly at the time instant 451.36 min in Figure 20. However the effect of the surfactant on our system was slow and therefore not the best surfactant for our particular rock fluids system. Table 18 is a summary of all the results obtained.

Table 18: Summary of results

Surfactant	Rank	PO Units	EO Units	T (min)	SD	t ₁ (min)	t ₂ (min)	θ_{af}	Wettability Alteration	IFT (mN/m)
ALFOTERRA G16-20S M	1	20	0	-	No	-	-	-	No	-
ALFOTERRA® S23-13S 90	2	13	0	34.4	Yes	94.42	458	150	No	0.016
ALFOTERRA® S23-11S 90	3	11	0	1.55	Yes	7.4	124.4	103	Yes	0.001
ALFOTERRA® S23-9S 90	4	9	0	7.18	Yes	12.40	405	90	Yes	0.012
ALFOTERRA® S23-7S 90	5	7	0	26.30	Yes	32.48	49.20	135	Yes	0.026
ALFOTERRA K3-41S	6	4	1	-	No	-	-	-	No	-
ALFOTERRA K45-DS	7	0	3	-	No	-	-	-	No	-

(Table 18 continued)

Surfactant	Rank	PO Units	EO Units	T (min)	SD	t ₁ (min)	t ₂ (min)	θ_{af}	Wettability Alteration	IFT (mN/m)
SOLOTERRA 960	1	4.5	2	54	Yes	434.47	435	-	No	0.030
SOLOTERRA 961	2	4.5	5	2.16	Yes	179.31	180	165	No	0.246
SOLOTERRA 939	3	1.6	2.4	18	No	-	-	-	No	0.300
SOLOTERRA 939	4	3	7	15.26	No	-	-	-	No	0.275
SOLOTERRA 939	5	0	7	9	Yes	23.17	25.16	160	Yes	0.380

T=Time for initial oil droplet to leave lower crystal

t₁=Time instance at which SD formation begins

t₂= Time instance at which SD formation ends

Θ_{af} = Final dynamic advancing contact angle measured

Θ_{ai} = Initial dynamic advancing contact angle measured = 148° – 152°

SD= Small droplet formation

5. CONCLUSIONS AND RECOMMENDATIONS

5.1 Conclusions

The objective of this study was to identify the effects of varying the structure of anionic surfactants on its potential to alter the wettability of a carbonate reservoir and in turn enhance the oil recovery. For our study we chose twelve different surfactants. Seven of them were alkyl alkoxy sulfates and belonged to the commercial line ALFOTERRA. The other five were alkyl ether carboxylates and belonged to the line of SOLOTERRA surfactants. Both family of surfactants were anionic in nature. Each of the surfactants in both the Alfoterra and Soloterra group differed from each other in their level of hydrophobicity. This was achieved by altering the number of propylene oxide (PO) and ethylene oxide (EO) units within the structure of the surfactant. All the surfactants were tested for their wettability altering potential on our selected system of Yates crude oil-Yates synthetic brine-Limestone. Dynamic water advancing contact angle measurements were made for each surfactant using the dual drop dual crystal (DDDC) technique for wettability measurement. The overall conclusions from this work are presented below.

1. The dynamic water advancing contact angle for our rock fluids system of Yates crude oil-Yates synthetic brine-Limestone was found to be 148°
2. Initial trials made with two selected Alfoterra surfactants at a concentration of 500 ppm resulted in the oil droplet between the two Limestone crystals escape within the first few seconds. The duration of the experiment lasted only minutes, with the maximum time amongst the two trial runs being 420 seconds.
3. Interfacial tension measurements made for the Alfoterras at a concentration of just 100ppm showed the IFT of our system reduced to in the range of $0.01\text{mN/m} - 0.001\text{mN/m}$. It was inferred that at 500 ppm, the interfacial activity of the Alfoterras was even higher and too

dominant in comparison to its possible wettability altering potential. Since wettability is not as instantaneous a phenomenon as IFT reduction, it was essential to give more time for our system and the surfactant to interact with each other. Therefore in order to increase the duration of our experimental time, the entire Alfoterra group of surfactants were tested at a 100 ppm concentration level.

4. Alfoterra G16-20S M (Hydrophobicity rank: 1, $PO(m) = 20$, $EO(n) = 0$) and Alfoterra K3-41S (Hydrophobicity rank: 6, $PO(m) = 4$, $EO(n) = 1$) & K45-DS (Hydrophobicity rank: 7, $PO(m) = 0$, $EO(n) = 3$) were found to be ineffective on the rock fluids system. The Yates oil drop between the two crystals remained stationary.
5. Alfoterra 13S, 11S, 9S and 7S (Hydrophobicity rank: 2, 3, 4 and 5 respectively) had an effect on our system. In each case the drop eventually left the lower crystal and escaped to the top crystal. However Alf 13S did not alter the wettability. The water advancing contact angle measured was 148° and the system continued to remain oil-wet. Alf 11S and 9S preferentially altered the wettability of the system from oil wet to intermediate wet while Alf 7S made the system weakly oil-wet.
6. Each of the four surfactant, Alf 13S, 11S, 9S and 7S, were introduced into the cell at the constant rate of 11 cc/min. However the time taken for the four surfactants to affect the initial Yates drop between the two crystals varied.
7. The time taken for the oil droplet to escape the lower crystal during injection of Alf 13S was 34.4 minutes. It drastically decreased to 1.55 min during injection of Alf 11S. It then slightly increased again to 7.18 min during injection of Alf 9S. With the injection of Alf 7S, the time went back up again to 26.30 minutes.

8. Since the four Alfoterra differ in their structure with respect to the number of propylene oxide with Alf 13S, 11S, 9S and 7S having 13, 11, 9 & 7 PO units respectively, it can be deduced that Alf 13S is too hydrophobic while Alf 7S is too hydrophilic to be effective in altering the rock fluids interactions for the system in terms of wettability. The hydrophobicity range exhibited by Alf 11S and 9S are most ideal for this particular rock fluid system.
9. An initial trial run of a Soloterra surfactant at 500 and 1000 ppm had no effect on our system. The drop remained stationary. Therefore surfactants belonging to the Soloterra group were then tested at a concentration level of 2000 ppm.
10. All five Soloterra were ineffective in altering the wettability of the system even at the high concentration level of 2000 ppm.
11. Interfacial tension measurements showed the IFT reduction by the Soloterra at 2000 ppm to be comparatively less than the Alfoterra at 100 ppm and was in the range of 0.25 mN/m – 0.38 mN/m.
12. The rock fluids interactions for our system were quantified by calculating the Bond number for the surfactants at various time instances. The Bond number took into consideration both the effect of reduced interfacial tension as well as the measured contact angle, thereby serving as an effective tool of comparison amongst the different surfactants.
13. Results from this study show there exists an ideal level of hydrophobicity for the system. Surfactants belonging to either extremes of the spectrum aren't effective. For Alfoterra as the propoxylation decreased, the hydrophobicity decreased and its wettability altering extent increased. However below a certain level of hydrophobicity, achieved by the introduction of ethylene oxide units, the extent of its wettability altering potential For Soloterras, the increased ethoxylation failed to enhance its wettability altering effects.

5.2 Recommendations

The tests and results compiled in this thesis form the very basis of this project aimed at understanding the effects of structural changes in surfactants and the possibility of optimizing a surfactant to meet the required characteristics for better recovery while making it economical as well. The following are recommendations that would help maintain the continuity of this project and help progress towards its goals.

1. Conduct and compare the effect of injection of the alkyl ether carboxylates (Soloterras) on a different carbonate system to see if the surfactant is ineffective on carbonates in general or just our system of Yates crude oil-Limestone-Yates synthetic brine, in particular.
2. Conduct adsorption tests for the alkyl ether carboxylates (Soloterra) and compare it to the adsorption tests for the alkyl alkoxy sulfates (Alfoterra). A low adsorption quotient for the Soloterra might be the reason for their inability to alter wettability even at high concentration levels.
3. Conduct the same experimental runs for all of the twelve surfactants by injecting them at the same concentration levels but on a sandstone reservoir system and compare the effects in terms of wettability. This in particular would be of importance to see the effect of these particular group of Soloterra, the ether carboxylates, on a sandstone system.
4. Conduct experimental runs for ALFOTERRA 13S, 11S, 9S 7S and all five SOLOTERRA at reservoir conditions of pressure, temperature and live oil composition.
5. Conduct core-floods using the 12 surfactants and do a comparative analysis of the wettability inferred from oil-wet relative permeability with contact angles and evaluate the effect of surfactant structure on wettability alterations and the consequent oil recovery enhancements.

REFERENCES

1. Adams, W. T., & Schievelbein, V. H. (1987). 12686 - Surfactant Flooding Carbonate Reservoirs. *SPE Reservoir Engineering*, 2(04), 619–626. <http://doi.org/10.2118/12686-PA>
2. Adkins, S., Liyanage, P., Pinnawala Arachchilage, G. W. P., Mudiyansele, T., Weerasooriya, U., & Pope, G. (2010). A New Process for Manufacturing and Stabilizing High-Performance EOR Surfactants at Low Cost for High-Temperature, High-Salinity Oil Reservoirs. *Proceedings of SPE Improved Oil Recovery Symposium*. <http://doi.org/10.2118/129923-MS>
3. Agbalaka, C., Dandekar, A. Y., Patil, S. L., Khataniar, S., & Hemsath, J. R. (2008). The Effect of Wettability on Oil Recovery: A Review. *SPE Asia Pacific Oil and Gas Conference and Exhibition*, 1–13. <http://doi.org/10.2118/114496-MS>
4. Alotaibi, M., Azmy, R., & Nasr-El-Din, H. (2010). Wettability Challenges in Carbonate Reservoirs. *SPE Improved Oil Recovery ...*, (April), 24–28. <http://doi.org/10.2118/129972-MS>
5. Anderson, W. G. (1986). Wettability Literature Survey Part 1: Rock/Oil/Brine Interactions and the Effects of Core Handling on Wettability. *Journal of Petroleum Technology*, (October), 1125–1144. <http://doi.org/10.2118/13932-PA>
6. Anderson, W. G. (1987). Wettability Literature Survey-Part 6: The Effects of Wettability on Waterflooding. *Journal of Petroleum Technology*, 39(12), 1605–1622. <http://doi.org/10.2118/16471-PA>
7. Arabia, S., & Box, P. O. (2011). Impact of Wettability Alteration on Recovery Factor. *Spe*, 149044(May), 15–18.
8. Ayirala, S. C., Vijapurapu, C. S., & Rao, D. N. (2006). Beneficial effects of wettability altering surfactants in oil-wet fractured reservoirs. *Journal of Petroleum Science and Engineering*, 52(1-4), 261–274. <http://doi.org/10.1016/j.petrol.2006.03.019>
9. Bobek, J. E., Mattax, C. C., & Denekas, M. O. (1958). Reservoir rock wettability—its significance and evaluation. *Trans. AIME*, 213, 155–160.
10. Causin, E., & Bona, N. (1994). In-Situ Wettability Determination: Field Data Analysis. *European Petroleum Conference*. <http://doi.org/10.2118/28825-MS>
11. Chen, H. L., Lucas, L. R., Nogaret, L. a D., Yang, H. D., Kenyon, D. E., & Company, M. O. (2000). SPE 59006 Laboratory Monitoring of Surfactant Imbibition Using Computerized Tomography, (February).
12. Chen, P., & Mohanty, K. K. (2014). SPE-169125-MS Wettability Alteration in High Temperature Carbonate Reservoirs, (April), 12–16. <http://doi.org/10.2118/166280-MS>

13. Dodd, C. G., & Aime, M. (n.d.). No . 1480 G The Problem of Determining Petroleum Reservoir Rock Wettability, (1480).
14. Duscha, S., Boukari, H., & Shcherbakov, D. (2014). Identification and Evaluation of, (April), 44–46. <http://doi.org/10.1128/mBio.01827-14>. Editor 66
15. Effects, N. (1955). Certain Wettability Effects In Laboratory Waterflood.
16. Fleureau, J. (1992). Wettability of reservoir core samples. SPE Formation Evaluation, (June), 132–138. <http://doi.org/10.2118/19681-PA>
17. Graue, a., Bognø, T., Baldwin, B. a., & Spinler, E. a. (2001). Wettability Effects on Oil-Recovery Mechanisms in Fractured Reservoirs. SPE Reservoir Evaluation & Engineering, 4(6), 3–6. <http://doi.org/10.2118/74335-PA>
18. Gupta, R., Mohan, K., & Mohanty, K. (2009). Surfactant Screening for Wettability Alteration in Oil-Wet Fractured Carbonates. Proceedings of SPE Annual Technical Conference and Exhibition, 1–21. <http://doi.org/10.2118/124822-MS>
19. Gupta, R., & Mohanty, K. K. (2010). Temperature Effects on Surfactant-Aided Imbibition Into Fractured Carbonates. SPE Journal, 15(3), 7–9. <http://doi.org/10.2118/110204-PA>
20. Hill, H. J., Reisberg, J., & Stegemeier, G. L. (1973). Aqueous Surfactant Systems For Oil Recovery. Journal of Petroleum Technology, 25(2). <http://doi.org/10.2118/3798-PA>
21. Hirasaki, G. J. (1991). Wettability: Fundamentals and Surface Forces. SPE Formation Evaluation, 6(02), 217–226. <http://doi.org/10.2118/17367-PA>
22. Hirasaki, G., Miller, C., & Puerto, M. (2011). Recent Advances in Surfactant EOR. SPE Journal, 16(4), 3–5. <http://doi.org/10.2118/115386-PA>
23. Hirasaki, G., & Zhang, D. (2004). Surface Chemistry of Oil Recovery From Fractured, Oil-Wet, Carbonate Formations. SPE Journal, 9(2), 5–8. <http://doi.org/10.2118/88365-PA>
24. Jürgenson, G. A., Bittner, C., Oetter, G., Se, B., & Corp, J. T. B. (2015). Alkyl Ether Carboxylate Surfactants for Chemically Enhanced Oil Recovery in Harsh Field Conditions.
25. Levitt, D. B. (2006). Experimental Evaluation of High Performance EOR Surfactants for a Dolomite Oil Reservoir. Engineering, 160.
26. Li, J., Wang, W., & Gu, Y. (2004). Dynamic Interfacial Tension Phenomenon and Wettability Alteration of Crude Oil-Rock-Alkaline-Surfactant Solution Systems. Spe90207.
27. Manrique, E., Gurfinkel, M., & Muci, V. (2004). Enhanced Oil Recovery Field Experiences in Carbonate Reservoirs in the United States EOR in U . S . Carbonate

Reservoirs. 25th Annual Workshop and Symposium Collaborative Project on Enhanced Oil Recovery International Energy Agency, 1–32.

28. Mitchell, a. G., Hazell, L. B., & Webb, K. J. (1990). Wettability Determination: Pore Surface Analysis. Proceedings of SPE Annual Technical Conference and Exhibition, 351–360. <http://doi.org/10.2523/20505-MS>
29. Morrow, N. (1990). Wettability and Its Effect on Oil Recovery. Journal of Petroleum Technology, 42(12), 1476–1484. <http://doi.org/10.2118/21621-PA> 67
30. Mugele, F., Siretanu, I., Kumar, N., Bera, B., Wang, L., Maestro, A., ... Collins, I. (2014). Charge Control And Wettability Alteration At Solid-liquid Interfaces. SPE Improved Oil Recovery Symposium, 1–14. <http://doi.org/10.2118/169143-MS>
31. Mungan, N. (1964). Role of Wettability and Interfacial Tension in Water Flooding. Society of Petroleum Engineers Journal, 4(02), 115–123. <http://doi.org/10.2118/705-PA>
32. Nelson, R. C., Lawson, J. B., Thigpen, D. R., & Stegemeier, G. L. (1984). Cosurfactant-Enhanced Alkaline Flooding. Spe/Doe 12672, 413. <http://doi.org/10.2118/12672-MS>
33. Rao, D. N. (2002). Measurements of dynamic contact angles in solid-liquid-liquid systems at elevated pressures and temperatures. Colloids and Surfaces A: Physicochemical and Engineering Aspects, 206(1-3), 203–216. [http://doi.org/10.1016/S0927-7757\(02\)00077-8](http://doi.org/10.1016/S0927-7757(02)00077-8)
34. Rao, D. N., & Girard, M. G. (1996). A new technique for reservoir wettability characterization. Journal of Canadian Petroleum Technology, 35(1), 31–39.
35. Sasol. (n.d.-a). EOR Brochure. Lake Charles: Sasol.
36. Sasol. (n.d.-b). Master EOR -section 2. Lake Charles: Sasol.
37. Sasol. (n.d.-c). Master EOR slides for update_section_3_v3. Lake Charles: Sasol.
38. Schramm, L. L. (2000). Surfactants: Fundamentals and applications in the petroleum industry. Cambridge University Press. [http://doi.org/10.1016/S1385-8947\(00\)00246-1](http://doi.org/10.1016/S1385-8947(00)00246-1)
39. Solairaj, S., Britton, C., Lu, J., Kim, D. H., Weerasooriya, U., & Pope, G. A. (2013). New Correlation to Predict the Optimum Surfactant Structure for EOR. SPE Improved Oil Recovery Symposium, 0(April), 2–11. <http://doi.org/10.2118/154262-MS>
40. Somasundaran, P., & Zhang, L. (2006). Adsorption of surfactants on minerals for wettability control in improved oil recovery processes. Journal of Petroleum Science and Engineering, 52(1-4), 198–212. <http://doi.org/10.1016/j.petrol.2006.03.022>
41. Waterflooding, D. (2012). Changes in Wettability State, 53(6), 420–429.

42. Webb, K. J., Black, C. J. J., & Namba, T. (1996). Resolving Wettability in a Giant Carbonate Reservoir. 7th Proceedings of Abu Dhabi International Petroleum Exhibition and Conference, 13-18 October. SPE 36257. <http://doi.org/10.2118/36257-MS>
43. Zheng, Y., & Rao, D. N. (2013). Surfactant-Induced Spreading and Wettability Effects in Condensate Reservoirs. SPE Improved Oil Recovery Symposium. <http://doi.org/10.2118/129668-MS>

VITA

Sandeep Gupta was born in Kolkatta, India to Mrs. Dipti Gupta and Dr. S. K. Gupta. He attended and graduated his high school from St. Joseph's Academy, Dehradun and went on to pursue a bachelor's degree in mechanical engineering from Manipal Institute of Technology, India. In Fall of 2013, Sandeep started his Master of Science degree at the Craft and Hawkin's Department of Petroleum Engineering at Louisiana State University and will graduate in Summer of 2016.